XANTHINE OXIDASE CONTRIBUTES TO MECHANICAL VENTILATION-INDUCED DIAPHRAGMATIC OXIDATIVE STRESS AND CONTRACTILE DYSFUNCTION

By

MELISSA ANN WHIDDEN

A DISSERTATION PRESENTED TO THE GRADUATE SCHOOL
OF THE UNIVERSITY OF FLORIDA IN PARTIAL FULFILLMENT
OF THE REQUIREMENTS FOR THE DEGREE OF
DOCTOR OF PHILOSOPHY

UNIVERSITY OF FLORIDA

2008

To my husband, family, and friends for their constant support and to the teachers and professors who have played a role in my education

ACKNOWLEDGMENTS

First, I thank my mentor Dr. Scott Powers for his guidance and continuous support during my graduate education. He is a great example as to the researcher I aspire to be. Also, I praise my supervisory committee members; Dr. Stephen Dodd, Dr. David Criswell and Dr. Glenn Walter for their direction and support throughout my graduate studies. I also thank Dr. Krista Vandenborne for presenting me the opportunity to be involved with an NIH T32 award. As a T32 trainee, I had the opportunity to expand my scientific career with meetings and workshops. Of course I wish to thank all laboratory members who have played a role in my achievements. Finally and most importantly, I am thankful for the experiences shared with my husband and family throughout my life and career.

TABLE OF CONTENTS

LIST OF TABLES

LIST OF FIGURES

Abstract of Dissertation Presented to the Graduate School
of the University of Florida in Partial Fulfillment of the
Requirements for the Degree of Doctor of Philosophy

XANTHINE OXIDASE CONTRIBUTES TO MECHANICAL VENTILATION-INDUCED DIAPHRAGMATIC OXIDATIVE STRESS AND CONTRACTILE DYSFUNCTION

By

Melissa Ann Whidden
May 2008

Chair: Scott K. Powers
Major: Health and Human Performance

Mechanical ventilation (MV) is used to mechanically assist or replace spontaneous breathing in patients who cannot sustain sufficient alveolar ventilation. The withdrawal of MV from patients is referred to as "weaning" and problems in weaning patients from MV are common. Unfortunately, MV results in the development of diaphragmatic atrophy and contractile dysfunction that likely contribute to weaning difficulties. Importantly, oxidative stress has been critically linked to the signaling events responsible for the progression of MV-induced diaphragmatic atrophy. However, the sources of oxidants in the diaphragm during MV have not been fully elucidated. An intracellular enzyme, xanthine oxidase (XO), is capable of producing reactive oxygen species (ROS) in skeletal muscle and we hypothesized that XO plays a key role in MV-induced oxidative stress in the diaphragm. To test this postulate, we mechanically ventilated rats for 12 or 18 hours (MV) with a subset of animals that combined MV along with a XO inhibitor, oxypurinol (MVO). Indices of XO activity and protein, oxidative stress, contractile function, and atrophy were measured in the diaphragm following the experimental protocol. Our study reveals that XO activity is elevated in the diaphragm during MV and oxypurinol provides protection against oxidative injury and contractile dysfunction. Specifically, oxypurinol administration attenuated protein oxidation and lipid peroxidation in the

diaphragm during MV. Further, XO inhibition attenuated MV-induced contractile dysfunction of the diaphragm at stimulation frequencies above 60 hertz at both 12 and 18 hours of MV. Together, these results reveal that XO-mediated production of oxidants is involved in MV-induced diaphragmatic oxidative stress and contractile dysfunction.

CHAPTER 1
INTRODUCTION

Mechanical ventilation (MV) is used clinically to defend pulmonary gas exchange in patients who are unable to sustain sufficient alveolar ventilation. Respiratory failure, spinal cord injury, drug overdose, and surgery are among the various conditions that render the pulmonary system unable to maintain blood gas homeostasis (30, 44). While MV supports ventilation in periods of respiratory distress, removal from the ventilator, termed weaning, is often difficult. In fact, problems in weaning patients from MV are common, whereby ~25% of the MV population has trouble weaning from the ventilator (70). Regrettably, weaning difficulties account for almost half of the total time spent on the ventilator (29), so understanding the mechanism(s) that contribute to weaning failure is imperative.

There is accumulating evidence that weaning problems are linked to inspiratory muscle dysfunction which results in the inability of the respiratory muscles to maintain adequate ventilation. Specifically, our laboratory has shown that respiratory muscle weakness produced by prolonged MV is due to diaphragmatic atrophy and contractile dysfunction (79, 80, 98, 108, 110). Moreover, we have demonstrated that MV-induced diaphragmatic contractile dysfunction is directly linked to oxidative stress (12, 31, 81, 110, 122, 132). The generation of reactive oxygen species (ROS) in the diaphragm during MV can damage proteins, lipids and DNA and interrupt normal cell signaling. In fact, oxidation of both actin and myosin occurs in the diaphragm within the first 6 hours of MV (132). This is significant because oxidation of contractile proteins contributes to abhorrent excitation-contraction coupling and decreased muscle force production (132). Therefore, it is necessary to identify the cellular pathways responsible for ROS production in the diaphragm during MV.

Numerous ROS producing pathways exist in skeletal muscle and they include; nicotinamide adenine dinucleotide phosphate (NAD(P)H) oxidase, nitric oxide synthase (NOS), heme-oxygenase-1 (HO-1), mitochondria, and xanthine oxidase (XO). With regards to MV, one or more of these pathways may contribute to the oxidative stress that is observed in the diaphragm. Our laboratory has already examined both the NOS and NAD(P)H oxidase pathways in the diaphragm and their contribution to ROS production during MV. Specifically, we revealed that MV-induced oxidative stress in the diaphragm is not due to increases in nitric oxide (122). Likewise, we have shown that NAD(P)H oxidase is not a substantial source of oxidant production in the diaphragm during prolonged mechanical ventilation (McClung et al., unpublished).

Therefore, we have focused on xanthine oxidase (XO) as a potential pathway involved in the formation of ROS in the diaphragm during MV. Xanthine oxidoreductase (XOR) is an intracellular enzyme that has been localized in the cytosol of skeletal muscle fibers (40, 49). XOR is involved in purine catabolism where the enzyme catalyzes the reduction of hypoxanthine and xanthine to uric acid (40, 42). Importantly, XOR exists in two interconvertible forms, xanthine dehydrogenase (XDH) and xanthine oxidase (XO) (39, 42, 130). In the dehydrogenase form, the enzyme utilizes nicotinamide adenine dinucleotide (NAD+) as its electron acceptor in purine catabolism. However, in the oxidase form, because molecular oxygen is used as the electron acceptor instead of NAD+, hypoxanthine and xanthine are reduced to uric acid and superoxide. Therefore, only the XO form is capable of producing ROS. In skeletal muscle, the level of superoxide production that occurs due to this pathway is dependent upon the levels of XO present and the ratio of XO to XDH in the fiber. Since XO produces superoxide and is found in skeletal muscle of both rats and humans (40, 42) it may contribute to ROS production in

the diaphragm during MV. Therefore, these experiments investigated the contribution of XO to ROS production in the diaphragm during MV and examined potential mechanism(s) by which XO may be activated in skeletal muscle. Our experiments were designed to achieve the following specific aims.

Specific Aim 1: To determine if pharmacological inhibition of XO activity in the diaphragm reduces MV-induced oxidative stress and contractile dysfunction.

Rationale: Our work indicates that MV results in diaphragmatic oxidative injury as a result of increased ROS production (12, 31, 80, 110, 122, 132). Despite the fact that there is significant evidence that XO plays an important role in oxidant production in diseased cardiac muscle (25, 27, 50, 68, 82, 103), it is unclear whether XO contributes to oxidant production in the diaphragm during MV.

Hypothesis: The administration of a XO inhibitor will attenuate diaphragmatic MV-induced oxidative stress and contractile dysfunction.

Specific Aim 2: To ascertain whether the administration of an exogenous antioxidant during MV maintains redox balance in the diaphragm and prevents XO activation.

Rationale: The oxidation of cysteine residues on the dehydrogenase form of XOR results in the reversible conversion of XDH to XO and subsequent XO activation (85, 101). Therefore, it is feasible that during MV, XO may be activated via oxidants produced from pathways other than XO. Previous work in our laboratory has shown that the administration of Trolox, a water-soluble Vitamin E analog, reduces both oxidative stress and contractile dysfunction in the diaphragm during MV (12, 80, 81). However, it is unknown whether Trolox administration reduces XO activation in the diaphragm during MV.

Hypothesis: Trolox administration during MV will maintain redox balance in the diaphragm and attenuate MV-induced XO activation.

Specific Aim 3: To determine if a ROS challenge (hydrogen peroxide) activates XO in skeletal muscle myotubes.

Rationale: In non-muscle cell lines, hydrogen peroxide (H_2O_2) has been shown to modulate the reversible conversion of XDH to XO (85), suggesting a possible role for free radical production via other pathways in the induction of XO activity. However, it is unknown whether hydrogen peroxide activates XO in skeletal muscle myotubes. By utilizing murine myotubes *in vitro,* we will examine the mechanism(s) by which XO is activated in skeletal muscle.

Hypothesis: Treatment of skeletal muscle myotubes with hydrogen peroxide will increase XO activity via the reversible conversion of XDH to XO.

CHAPTER 2
LITERATURE REVIEW

Mechanical ventilation (MV) is used to achieve satisfactory pulmonary gas exchange in patients incapable of maintaining adequate alveolar ventilation. The withdrawal of MV from patients is referred to as "weaning" and problems in weaning from MV are common. Numerous studies indicate that MV-induced diaphragmatic weakness, due to both atrophy and contractile dysfunction, is an important contributor to weaning difficulties.

Although the specific mechanisms responsible for MV-induced diaphragmatic weakness remain unknown, it is now clear that oxidative stress in the diaphragm plays a major role in regulating the signaling processes leading to MV-induced diaphragmatic dysfunction. It follows that understanding the sources of oxidant production in the diaphragm during prolonged MV is important. Hence, this forms the rationale for the experiments contained within this dissertation. Specifically, our experiments were designed to investigate the role that a specific oxidant production pathway (i.e. xanthine oxidase) plays in MV-induced oxidative injury in the diaphragm.

This chapter will discuss the importance of our experimental work and will develop the ideas behind our hypotheses based upon our prior research and the work of others. Specifically, this review will be divided into two concise segments: 1) an overview of MV-induced diaphragmatic injury; and 2) a detailed discussion of oxidant producing pathways in skeletal muscle.

Overview of Mechanical Ventilation-Induced Diaphragmatic Injury

Introduction

Mechanical ventilation (MV) is used clinically for patients with respiratory distress. Specifically, when an individual is unable to sustain adequate alveolar ventilation on their own,

MV is required to maintain adequate gas exchange. Unfortunately, problems in weaning patients from MV are common (70). Failure to wean patients from MV is a problem because increased time on the ventilator increases complications and the incidence of morbidity and mortality outcomes (17, 70, 121, 125, 126). In addition, longer stays in the intensive care unit for extra weaning time result in excess health care costs (70). Thus, the identification of the mechanism(s) responsible for MV-induced diaphragmatic weakness is imperative.

Diaphragm Response to Mechanical Ventilation

Our laboratory has extensively examined MV in a rat model. We have documented the changes that occur in the diaphragm muscle that likely contribute to respiratory muscle weakness and weaning difficulties. Our findings are presented in Table 2-1 in a time course dependent manner (12, 23, 31, 79-81, 98, 108-110, 122, 123, 132). While our laboratory uses a rat model of MV, there is abundant evidence from other animal models (rabbits, pigs, and baboons) along with recent data from human research that support the concept that prolonged MV results in diaphragmatic dysfunction (4, 10, 32-34, 51, 69, 71, 93, 99, 100, 104-106, 124, 129, 131, 133). Collectively, these studies clearly document the damaging effects of MV on the diaphragm.

While all animal models of MV report a wide array of detrimental effects on the diaphragm, limited human MV studies exist. Because of the invasive nature of obtaining a biopsy from a human diaphragm, human MV studies are difficult to conduct. However, a recent study demonstrates that prolonged MV results in diaphragmatic atrophy in humans (71). Specifically, Levine et al. observed an approximate 40% decrease in cross-sectional area across both type I and type IIa diaphragm fibers in patients ventilated between 18-72 hours (71). In another human study, investigators found that twitch transdiaphragmatic pressure in individuals with disease was 50% lower than healthy patients following MV (129). Finally, a retrospective

analysis of postmortem data obtained from neonates who received ventilatory assistance for 12 days or more reported diffuse diaphragmatic fiber atrophy, which was not observed in locomotor muscles (58).

Mechanisms of Diaphragmatic Dysfunction

Contractile dysfunction

Problematic weaning is often associated with respiratory muscle weakness. In baboons, Anzueto and colleagues demonstrated a decrease in both maximal diaphragmatic force production and endurance after 11 days of MV (4). In a rat model of MV, Le Bourdelles et al. documented a significant 60% reduction in maximal diaphragmatic specific force following 48 hours of MV (69). Our laboratory has shown that the MV-induced decline in diaphragmatic submaximal and maximal specific force increases as a function of time on the ventilator (Figure 2-1) (98). Specifically, maximal diaphragmatic specific force is approximately 18% and 46% lower in animals ventilated for 12 and 24 hours respectively, when compared to control animals (98).

Atrophy

MV-induced diaphragmatic atrophy has been observed in both animal and human experiments (4, 10, 33, 58, 69, 71, 79, 80, 110, 131). While atrophy occurs during many types of skeletal muscle disuse, the rate of atrophy during MV is extraordinarily fast when compared with hindlimb muscle unloading (69, 79, 131). For example, only 12 hours of MV results in a significant reduction in diaphragmatic myofiber size. Work by Shanley et al. revealed a 15–30% reduction in myofiber cross-sectional area across all four fiber types in the rat diaphragm following 18 hours of MV (110). To achieve this level of atrophy in hindlimb skeletal muscle, muscles would need to be unloaded for more than 96 hours (120). As mentioned above, Levine

and colleagues found a similar reduction in myofiber size in the human diaphragm following 18–72 hours of MV (71).

Protein synthesis and degradation

Diaphragmatic atrophy can result from a decline in protein synthesis (66) and/or an increase in protein degradation (13). The decrease in protein synthesis often observed in models of skeletal muscle disuse is characterized by alterations in translational initiation and elongation and/or a decrease in cellular RNA (48, 66, 89, 90). Our laboratory has observed a decrease in protein synthesis in as few as 6 hours following MV (109). With respect to the protein synthetic signaling pathway, McClung and colleagues found that MV increases the activation of the translational repressor protein 4E-BP1 and decreases the activity of the translational initiation factor p70s6kinase (81). Both the increase in 4E-BP1 and the decrease in p70s6kinase signify early events in skeletal muscle atrophy (81). When protein synthesis is reduced and myofiber myosin heavy chain content is minimized during MV, diaphragmatic atrophy ensues. Nevertheless, although MV results in decreased protein synthesis in the diaphragm our laboratory has demonstrated that the development of atrophy during MV is primarily due to an increase in protein degradation (23, 80, 81, 110).

There are several proteolytic systems that contribute to skeletal muscle degradation during MV, including the lysosomal, calpain, caspase-3, and proteasome pathways (8, 97, 127). While currently it is not known whether the lysosomal pathway plays a major role in MV-induced atrophy (reviewed in 97), both calpain and caspase proteases are believed to cleave proteins that anchor the contractile elements to the myofilament (19). Thus, during MV, calpain and caspase-3 activation may act as the initial step in muscle protein loss during diaphragmatic atrophy. Following the release of myofibrillar proteins, the ubiquitin proteasome pathway appears to be

the major proteolytic system responsible for skeletal muscle protein degradation. Protein degradation by this pathway involves substrate recognition via the coordinated action of a three-enzyme system and protein degradation by the 26S proteasome (23). Our laboratory has shown that MV increases diaphragmatic levels of two ubiquitin ligases and increases 20S proteasome activities including chymotrypsin and trypsin-like activities (23).

Oxidative stress

ROS are produced in inactive skeletal muscles and oxidative stress-induced cellular injury can contribute to muscle atrophy (23, 61-65). Since the diaphragm muscle is completely inactive during controlled MV (98, 106) , the potential for ROS production exists. In skeletal muscle, when ROS production exceeds the antioxidant capacity, oxidative stress occurs (96). We have shown that within 6 hours after the initiation of MV, oxidative injury in the diaphragm occurs (132). Oxidative stress can alter the structure, function and/or regulation of lipids, proteins, and DNA in the cell. Therefore, it is important to identify the sources of ROS that contribute to redox imbalances in the muscle cell. Numerous ROS producing pathways exist in the cell (Figure 2-2) and they include; 1) nicotinamide adenine dinucleotide phosphate (NAD(P)H) oxidase, 2) nitric oxide synthase (NOS), 3) heme oxygenase-1 (HO-1), 4) mitochondria, and 5) xanthine oxidase (XO). A brief overview of each of these pathways follows.

NAD(P)H Oxidase. NAD(P)H oxidase is a membrane-associated enzyme that catalyzes the one-electron reduction of molecular oxygen into superoxide using either NADH or NADPH as the electron donor (52). It has been shown that the calcium-sensitive PKC-ERK1/2 pathway can activate NAD(P)H oxidase activity in cells (41). While our laboratory has found that NAD(P)H oxidase inhibition via apocynin reduces MV-induced oxidative stress and contractile dysfunction, diaphragmatic NAD(P)H oxidase activity is only increased 4% during MV when compared with controls (McClung et al., unpublished). Although the contribution of NAD(P)H

oxidase to MV-induced oxidative stress appears to be small, it may act as an up-stream regulator of other pathways that generate ROS. Thus, NAD(P)H oxidase inhibition could reduce both MV-induced oxidative stress and contractile dysfunction by down-regulating other ROS producing pathways.

Nitric Oxide Synthase. Three isoforms of NOS exist (54, 112), however, only neuronal NOS (nNOS) and endothelial NOS (eNOS) are expressed in diaphragm muscle (54, 112, 122). Endogenous nitric oxide production via NOS can result in the formation of reactive nitrogen species, including peroxynitrite ($ONOO^-$). Reactive nitrogen species are associated with cellular injury including mitochondrial dysfunction, lipid peroxidation, and nitrosylation of proteins (7, 112, 118). In reference to MV-induced oxidative stress in the diaphragm muscle, Van Gammeren et al. demonstrated that nitric oxide is not involved in MV-induced oxidative injury in the diaphragm (122).

Heme Oxygenase-1. Heme oxygenase-1 (HO-1) is an intracellular enzyme localized in the microsomal fraction of the cell (55). HO-1 catalyzes the rate-limiting step in the degradation of heme resulting in the generation of carbon monoxide, biliverdin, and free iron (119). Biliverdin can then be further reduced to bilirubin. Since bilirubin posses the ability to quench singlet oxygen, scavenge hypochlorous acid, and inhibit lipid peroxidation (18), the possibility of radical formation exists due to the release of free iron. Transitional metal ions such as iron are capable of converting superoxide and hydrogen peroxide to the highly reactive hydroxyl radical (67). However, our laboratory has recently shown that HO-1 acts as an antioxidant in the diaphragm by demonstrating that hemin-induced overexpression of HO-1 is associated with reduced oxidative stress during MV (Falk et al., unpublished). More importantly, HO-1

inhibition in the diaphragm during MV does not alter the normal progression of MV-induced oxidative stress (Falk et al., unpublished).

Mitochondrial oxidants. While the primary function of the mitochondria is to produce ATP, electron 'leak' from the electron transport chain may occur at complexes I and III resulting in the formation of superoxide and subsequently hydrogen peroxide (3, 16, 96). However, Fredriksson and colleagues observed negligible mitochondrial damage in the diaphragm following 5 days of MV (32). Nonetheless, due to the limited evidence, the role of mitochondrial generated oxidants in the diaphragm during MV should be further investigated.

Xanthine Oxidase. Xanthine oxidoreductase (XOR) is an intracellular enzyme localized primarily in the cytosol and it is involved in purine catabolism (40). XOR occurs as a homodimer and each subunit contains four redox centers; a molybdenum cofactor, a flavin adenine dinucleotide (FAD), and two iron sulfur cluster sites (15, 40, 46). Mammalian XOR catalyzes the hydroxylation of hypoxanthine and xanthine to uric acid at the molybdenum center of the enzyme. Reducing equivalents introduced into the enzyme are transferred via the two iron sulfur cluster sites to the FAD cofactor where the reduction of nicotinamide adenine dinucleotide (NAD+) or molecular oxygen occurs (60). Importantly, XOR exists in two interconvertible forms, xanthine dehydrogenase (XDH) and xanthine oxidase (XO) (39, 42, 130). XDH utilizes NAD+ as its electron acceptor in purine catabolism. However, XO uses molecular oxygen as its electron acceptor instead of NAD+, so hypoxanthine and xanthine are reduced to uric acid and superoxide ($O_2^{\cdot -}$) (shown below) (130). Therefore, only the XO form is capable of producing ROS.

$$\text{Hypoxanthine} + O_2 \xrightarrow{\text{XO}} \text{Xanthine} + O_2^{\cdot -} \qquad \text{Xanthine} + O_2 \xrightarrow{\text{XO}} \text{Uric acid} + O_2^{\cdot -}$$

The two forms of XOR (XDH and XO) can be interconverted reversibly by sulfhydryl oxidation or irreversibly by proteolysis of XDH to XO (1, 9, 11, 22, 25, 27, 40, 50, 84, 85, 92, 101, 102, 113, 114, 130). XOR is initially synthesized as a 150 kDa protein from which both XDH and XO are derived (85, 130). XDH only exists as the 150 kDa band of XOR while XO can be reflected in the 150 kDa band as well as an active 130 kDa band of XOR. The mechanisms responsible for the reversible or irreversible conversion of XDH to XO are not completely understood. Under baseline conditions, the majority of the 150 kDa protein contains XDH activity. Reversible formation of XDH to XO can be achieved by the oxidation of cysteine residues on XOR, a process that changes enzymatic function but not molecular weight (Figure 2-3) (85, 101). It is feasible that during MV, diaphragmatic XO activity could be up-regulated via the oxidation of XDH to XO. As mentioned above, pathways other than XO may generate ROS during prolonged MV and production of oxidants from one or more of those pathways may result in the oxidation of XDH. The subsequent XO activation and further ROS production through purine catabolism would contribute to oxidative damage in the diaphragm during MV.

Further, it is also possible that XO activation during MV may occur through the proteolytic conversion of XDH to XO (22, 27, 85, 101, 102, 113, 114, 130). The irreversible proteolysis of XDH occurs at a specific site leading to the formation of an active 130 kDa form of XO (Figure 2-3) (130). While the protease responsible for this conversion has been examined by investigators since the late 1960's, debate continues as to the specific identity of this protease (22, 102, 113, 114, 130). While some investigations suggest that a calpain-independent calcium (Ca^{2+}) activated protease functions in the cleavage of XDH to XO (1, 92, 102, 113), it has also been theorized that calpain is responsible for the cleavage in various tissues (39, 42). Since

calpain activity is increased in the diaphragm during MV (110), it is a potential candidate for the protease responsible for the cleavage.

Attention was first directed towards XO when Granger and colleagues examined the role of XO-derived ROS production in ischemia-reperfusion injury (37, 38, 82). These researchers found that during the course of ischemia, transmembrane ion gradients were dissipated allowing elevated cytosolic concentrations of calcium into the cell. The increase in intracellular calcium activated a protease that irreversibly converted XDH into XO. At the same time, cellular ATP was catabolized to hypoxanthine which accumulated over the duration of ischemia. Upon reperfusion and the restoration of oxygen, hypoxanthine was reduced to uric acid, superoxide, and hydrogen peroxide (37, 38, 82). Since then several studies have examined the role of XO-mediated ROS production in other tissues under varying physiological states (1, 11, 25, 28, 36, 42, 43, 45, 50, 53, 56, 68, 78, 84, 103, 117, 128). In doing so, these studies have used allopurinol or oxypurinol to effectively inhibit XOR activity. Allopurinol (1,5-dihydro-4H-pyrazolo (3,4-d) pyrimidine-4-one) is a structural analogue of hypoxanthine and inhibitor of xanthine oxidoreductase (88). It has a half-life of approximately 2 hours and is quickly metabolized to oxypurinol which has a half-life of ~18-30 hours (88).

In cardiac tissue XO has been found to contribute to abnormal excitation-contraction (EC) coupling and cardiac remodeling in heart failure (103). For instance, Saliaris and colleagues found that XO inhibition preserved the positive inotropic effects of dobutamine that were lost during heart failure (103). Likewise, Isabelle et al. found that XO inhibition prevents the myocardial production of superoxide anions in cocaine-induced left ventricular dysfunction in male rats (50). In this model, XO inhibition prevented cocaine-induced cardiac alterations by restoring cardiac output, stroke volume, and fractional shortening (50). Finally, in an

atherosclerosis study, McNally et al. reported that XO is responsible for increased ROS production in response to oscillatory shear stress that occurs at sites of circulation that are vulnerable to disease (84).

Recent evidence indicates that XO is found in skeletal muscle fibers of humans (42). In a study by Vina and colleagues, they found that XO is responsible for the free radical production and tissue damage that occurs during exhaustive exercise in humans (128). In COPD patients, XO inhibition reduced both glutathione oxidation and lipid peroxidation during strenuous exercise (45). Finally, it has been shown that XO contributes to oxidant production in the diaphragm during contraction (115). However, the XO pathway has not been studied with regard to oxidant production in the diaphragm during MV. This important void forms the basis for the current experiments.

Summary

Our laboratory has developed a rat animal model for the study of MV-induced atrophy and contractile dysfunction of the diaphragm muscle (12, 20, 79, 80, 98, 108, 110). By utilizing aseptic techniques and maintaining blood gas homeostasis, we have repeatedly demonstrated that this is an excellent animal model for examining the mechanisms that contribute to diaphragmatic injury during MV. Our laboratory has investigated the effects of oxidative stress, proteolysis, and atrophy on diaphragm myofiber function during various durations of MV. However, the oxidant pathways that contribute to MV-induced oxidative injury in the diaphragm are currently unknown. Since XO can generate superoxide in the presence of oxygen and the purine substrates, determining if XO contributes to MV-induced oxidative stress in the diaphragm is important and may lead to a therapeutic strategy to alleviate MV-induced diaphragmatic injury.

Table 2-1. Summary of MV-induced changes in the diaphragm observed during 3–24 hours of MV.

Measurement	3 hrs	6 hrs	12 hrs	18 hrs	24 hrs
Oxidative stress	↔	↑	↑	↑	ND
Caspase-3 activity	ND	↑↑	↑	ND	ND
Protein synthesis	ND	↓	↓	↓↓	ND
Protein degradation	ND	↑	↑	↑	ND
Contractile dysfunction	ND	ND	↑	↑	↑↑
Atrophy	ND	↔	↑	↑↑	ND
Myonuclear apoptosis	ND	↑	↑↑	ND	ND

ND; no data available, ↔; not significantly different from control value, ↑; increased vs. control value, ↑↑; further increased, ↓; decreased vs. control value, and ↓↓; further decreased. Data are from references (12, 23, 31, 79-81, 98, 108-110, 122, 123, 132).

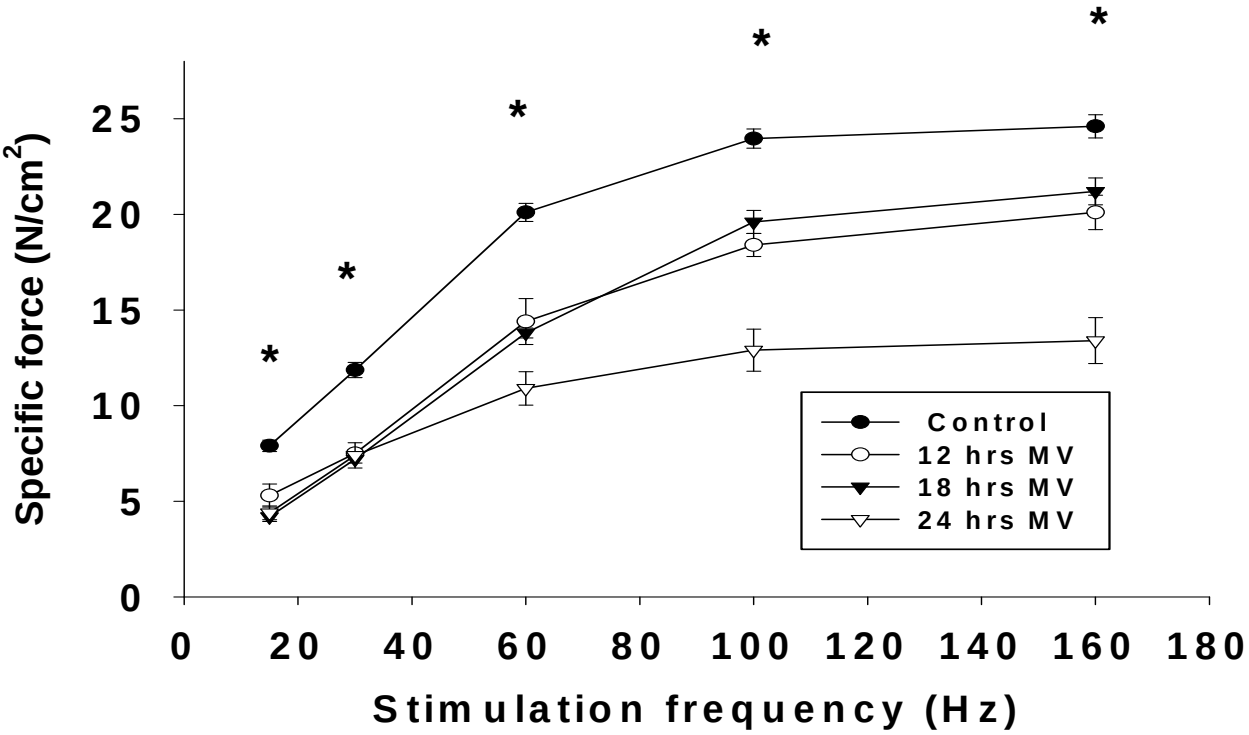

Figure 2-1. Effects of prolonged MV on the diaphragmatic force-frequency response (*in vitro*) in rats. Values are means ± SE. Compared with control, MV (all durations) resulted in a significant ($^{*}P < 0.05$) reduction in diaphragmatic specific force production at all stimulation frequencies (Redrawn from 98).

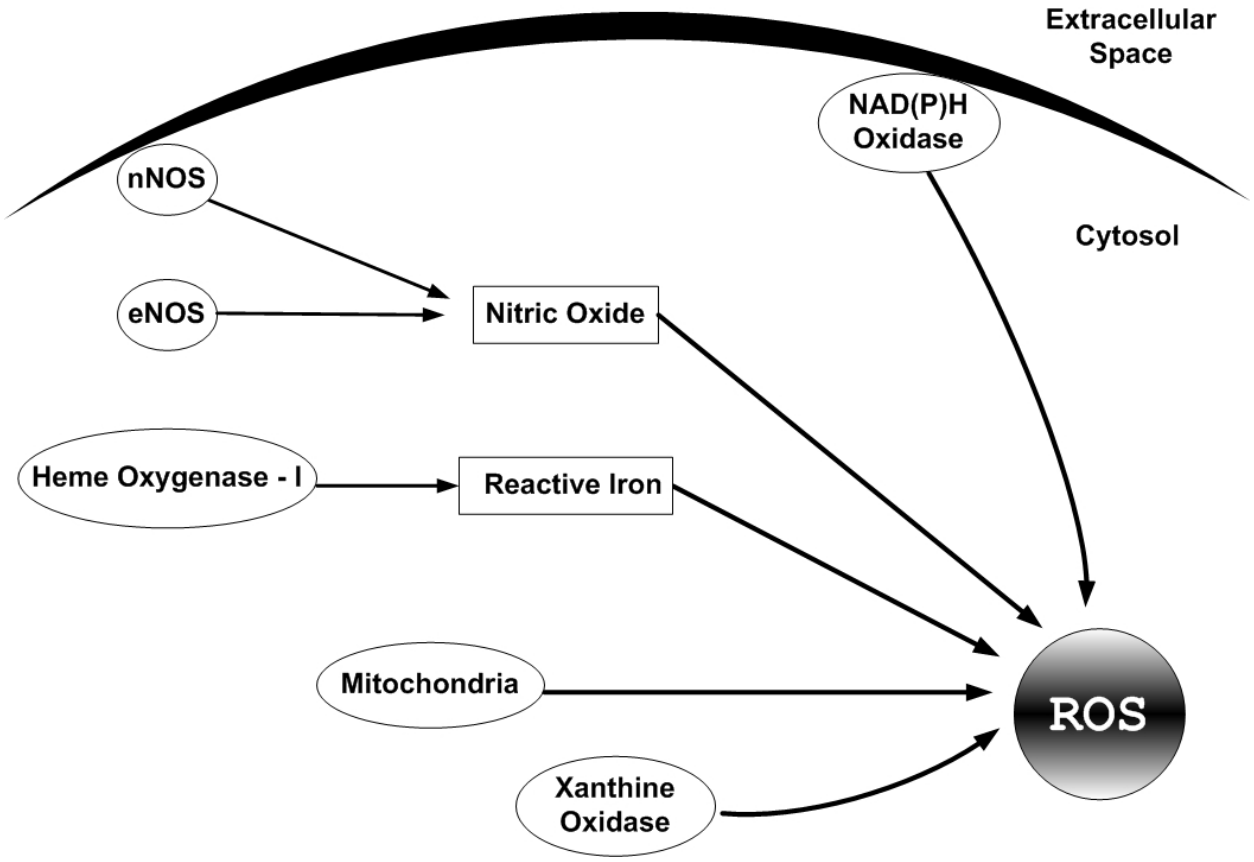

Figure 2-2. Potential sources of ROS production in the diaphragm during MV. Prolonged MV may cause an increase in one or more of the following sources of oxidants in the diaphragm: 1) NAD(P)H oxidase, 2) nitric oxide synthase, 3) heme oxygenase-1, 4) mitochondria, and 5) xanthine oxidase. Through these mechanisms, MV may cause an increase in the level of oxidative stress and subsequent injury to the diaphragm.

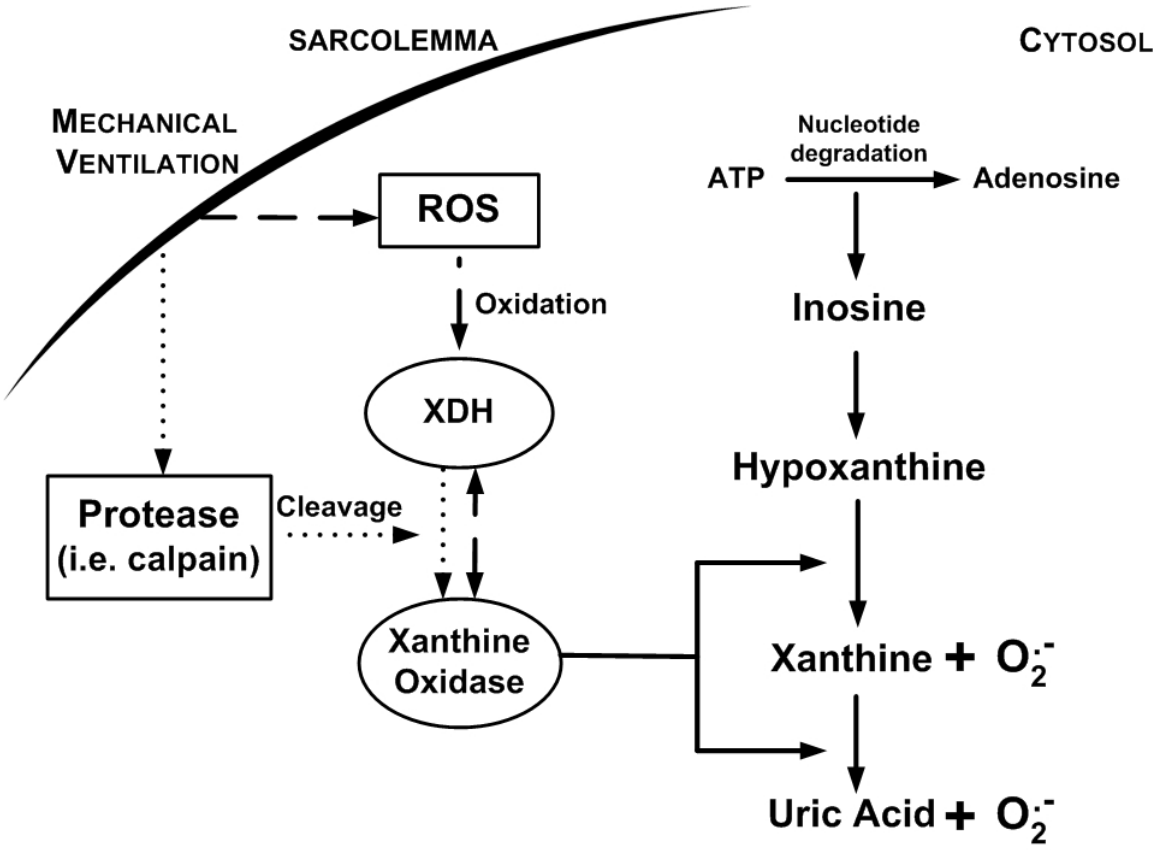

Figure 2-3. Two proposed mechanisms of XO activation in the diaphragm during MV. 1) MV can activate ROS-producing pathways that result in the oxidation and reversible conversion of XDH to XO (dashed arrows). 2) MV can activate a cellular protease that can irreversibly cleave XDH to XO (dotted arrows). Following either activation mechanism, XO catalyzes the reduction of hypoxanthine to xanthine and superoxide ($O_2^{\cdot-}$) and subsequently reduces xanthine to uric acid and additional superoxide ($O_2^{\cdot-}$).

CHAPTER 3
MATERIALS AND METHODS

This chapter will be divided into two sections. Section one includes the experimental designs used in each of our experiments that are intended to determine if XO contributes to oxidative stress and contractile dysfunction during MV and establish the mechanism(s) by which XO is activated in the diaphragm. In the subsequent section, we will provide the methodological details associated with each experimental protocol and measurement technique.

Experiment 1: Animals

Animal Model Justification

To address our first specific aim and determine if the pharmacological inhibition of XO activity in the diaphragm reduces MV-induced oxidative stress and contractile dysfunction, we used adult (4-6 month old) female Sprague-Dawley (SD) rats in experiment 1. The animals were 4-6 months of age (young adult) at the time of sacrifice. The SD rat was chosen due to the similarities between the rat and human diaphragm in both anatomical and physiological parameters (5, 6, 86, 87, 94, 95).

Animal Housing and Diet

All animals were housed at the University of Florida Animal Care Services Center according to guidelines set forth by the Institutional Animal Care and Use Committee. The Animal Care and Use Committee of the University of Florida has approved these experiments. Animals were maintained on a 12:12 hour reverse light-dark cycle and provided food (AIN93 diet) and water *ad libitum* throughout the experimental period.

Experimental Design

In experiment 1, adult rats were randomly assigned to one of the following groups; 1) acutely anesthetized control (CON) (n = 8), 2) acutely anesthetized control with oxypurinol

(CONO) (n = 8), 3) 12 hours of MV (12MV) (n = 8), 3) 12 hours of MV with oxypurinol (12MVO) (n = 8), 4) 18 hours of MV (18MV) (n = 8), and 5) 18 hours of MV with oxypurinol (18MVO) (n = 8) (Figure 3-1).

Animal Protocol

Animals in the control groups were acutely anesthetized with an intraperitoneal (i.p.) injection of sodium pentobarbital (60 mg/kg). After reaching a surgical plane of anesthesia, the control animals were sacrificed immediately and a section of the costal diaphragm was used for contractile measurements while the rest was stored at –80°C for subsequent analyses.

Animals in the MV groups were acutely anesthetized with sodium pentobarbital (60 mg/kg IP). After reaching a surgical plane of anesthesia, the animals were tracheostomized utilizing aseptic techniques and mechanically ventilated with a controlled pressure-driven ventilator (Seimens) for 12 or 18 hours with the following settings: upper airway pressure limit: 20 cmH_2O, PEEP: 1 cmH_2O, pressure control level above PEEP: 4-6 cmH_2O, and respiratory rate: 80 bpm (12, 123). We choose 12 and 18 hours of mechanical ventilation in order to establish a time course for these measurements because these periods of MV are associated with diaphragmatic oxidative stress, contractile dysfunction, and myofiber atrophy.

Animals in the oxypurinol groups (CONO, 12MVO, and 18MVO) received two intraperitoneal injections of oxypurinol (25 mg/kg body weight) 24 hours prior to treatment. Further, an additional 25 mg/kg body weight was administered via an i.p. injection 12–18 hours prior to sacrifice in the CONO animals and via infusion over a 10 min period before the initiation of MV in the 12MVO and 18MVO groups. This protocol has been reported to effectively inhibit XO activity in rat skeletal muscle (57). Animals in the MV group received an i.p. injection of saline and surgical preparation, procedures, and animal monitoring were performed as previously

described (31). Following the completion of each experimental protocol, the animals were immediately sacrificed and a section of the costal diaphragm was used for contractile measurements while the rest was stored at –80°C for subsequent analyses.

Statistical Analysis

Group sample size was determined using a power analysis of preliminary data from our laboratory. Comparisons between groups were made by a one-way ANOVA and, when appropriate, a Tukey HSD test was performed. Significance was established at $P < 0.05$.

Experiment 2: Animals

Animal Model Justification

To address our second specific aim and to ascertain whether the administration of an exogenous antioxidant during MV prevents diaphragmatic XO activation, adult (4-6 month old) female Sprague-Dawley (SD) rats were used for experiment 2. The animals were 4–6 months of age (young adult) at the time of sacrifice. The rationale for selecting the rat as an experimental model was discussed previously.

Animal Housing and Diet

All animals were housed at the University of Florida Animal Care Services Center according to guidelines set forth by the Institutional Animal Care and Use Committee. The Animal Care and Use Committee of the University of Florida has approved these experiments. Animals were maintained on a 12:12 hour reverse light-dark cycle and provided food (AIN93 diet) and water *ad libitum* throughout the experimental period.

Experimental Design

In experiment 2, adult rats were randomly assigned to one of the following groups; 1) acutely anesthetized control (CON) (n = 8), 2) 12 hours of MV (12MV) (n = 8), and 3) 12 hours of MV with Trolox (12MVT) (n = 8) (Figure 3-2).

Animal Protocol

Animals in the control group were acutely anesthetized with an intraperitoneal injection of sodium pentobarbital (60 mg/kg). After reaching a surgical plane of anesthesia, the control animals were sacrificed immediately and a section of the costal diaphragm was used for contractile measurements while the rest was stored at –80°C for subsequent analyses.

Animals in the MV groups were acutely anesthetized with sodium pentobarbital (60 mg/kg IP). After reaching a surgical plane of anesthesia, the animals were tracheostomized utilizing aseptic techniques and mechanically ventilated with a controlled pressure-driven ventilator (Seimens) for 12 hours with the following settings: upper airway pressure limit: 20 cmH_2O, PEEP: 1 cmH_2O, pressure control level above PEEP: 4-6 cmH_2O, and respiratory rate: 80 bpm (12, 123).

Animals in the Trolox group (12MVT) received an infusion of Trolox (20 mg/kg) over a 5-minute period, 20 minutes prior to the start of MV. Additionally, Trolox was infused continuously at a rate of 4 mg/kg per hour for the entirety of the ventilation treatment. We have previously used this protocol to effectively maintain redox balance in the diaphragm during MV (12, 80, 81) Animals in the MV group received an i.p. injection of saline and surgical preparation, procedures, and animal monitoring were performed as previously described (31). Following the termination of each experimental group, the animals were immediately sacrificed

and a section of the costal diaphragm was used for contractile measurements while the rest was stored at –80°C for subsequent analyses.

Statistical Analysis

Group sample size was determined using a power analysis of preliminary data from our laboratory. Comparisons between groups were made by a one-way ANOVA and, when appropriate, a Tukey HSD test was performed. Significance was established at $P < 0.05$.

Experiment 3: Cell Culture

To answer our third specific aim and determine if a ROS challenge activates XO in skeletal muscle myotubes, we used the C_2C_{12} myogenic cell line for experiment 3. The C_2C_{12} myogenic cell line was chosen because of the biochemical and functional similarities between these myotubes and rodent skeletal muscle fibers (26, 35, 72, 74-76). Cells were maintained in a temperature and gas controlled incubator throughout the experiments.

Experimental Design

In experiment 3, an independent observation was made by placing cells in one of the following groups; 1) no treatment (CON) (n = 6), 2) hydrogen peroxide (H_2O_2) (n = 6), 3) leupeptin (LEU) (n = 6), 4) hydrogen peroxide and leupeptin (H_2O_2 + LEU) (n = 6), 5) siRNA for calpain-1 (Cal-1 siRNA) (n = 6), and 6) hydrogen peroxide and siRNA for calpain-1 (H_2O_2 + Cal-1 siRNA) (n = 6) (Figure 3-3).

Cell Protocol

Myogenic cells were cultured according to Li (73). Briefly, myotubes were cultured in DMEM supplemented with 10% fetal bovine serum and gentamicin at 37ºC in the presence of 5% CO_2. Myoblast differentiation was initiated by replacing the growth medium with differentiation medium supplemented with 2% horse serum. Differentiation was allowed to

continue for 96 hours before experimentation, changing to fresh media every 24 hours. At the time of harvest, myotubes were washed 3x in PBS buffer (pH 7.4) before the addition of cell lysis buffer. After the addition of lysis buffer, myotubes were collected and centrifuged at 1100 *g* for 10 min at 4°C. The supernatant was collected and stored at –80°C for subsequent analyses.

We chose 100 μM hydrogen peroxide (H_2O_2) for the oxidative challenge in these experiments. This concentration of H_2O_2 has been used in the literature in order to induce a stress response in C_2C_{12} myotubes (74, 116). In addition, this concentration may have relevance to *in vivo* cellular levels. Therefore, we chose this concentration to induce oxidative stress in the C_2C_{12} cells. H_2O_2 treatment was administered 4 hours prior to harvest in the hydrogen peroxide, hydrogen peroxide plus leupeptin, and the hydrogen peroxide plus siRNA for calpain-1 cell groups. We choose 4 hours for our incubation period because preliminary data showed that while XO activation was induced in our cell line following H_2O_2 treatment for 1 hour, XO activity was significantly increased following the 4 hour incubation period.

Myotubes in the leupeptin (LEU) groups were cultured in horse serum combined with 120 μM leupeptin and were incubated for 4 hours alone or in combination with H_2O_2 prior to harvest. Leupeptin was selected as a general calpain inhibitor to examine the irreversible proteolytic conversion of XDH to XO. We choose 120 μM leupeptin for these experiments because this concentration has been shown to effectively inhibit calpain activity in C_2C_{12} cells (21).

Lastly, myotubes in the short interference RNA (siRNA) groups were grown in horse serum and were transfected with siRNA for calpain-1 three days prior to harvest or the addition of H_2O_2. We included siRNA for calpain-1 as another means to effectively inhibit calpain activity however siRNA was specific for calpain-1 activity. We have previously shown that

siRNA for calpain-1 reduces calpain-1 mRNA by 65% and active calpain-1 protein levels by 53% in the C_2C_{12} cell line (unpublished observation).

Statistical Analysis

Group sample size was determined using a power analysis of preliminary data from our laboratory. Comparisons between groups were made by a one-way ANOVA and, when appropriate, a Tukey HSD test was performed. Significance was established at $P < 0.05$.

General Methods

Animal Measurements

Histological

Immunohistochemistry. Diaphragm samples were removed and fixed in OCT and stored at –80°C. On the day of analysis, sections from frozen diaphragm samples were cut at 10 microns with a cryotome (Shandon Inc., Pittsburgh, PA) and allowed to air dry at 25°C for 30 minutes. Slides were fixed in acetone (4°C) for 5 minutes and allowed to air dry for an additional 30 min at 25ºC. Slides were washed 2 times for 2 minutes in phosphate buffered saline (PBS) and then blocked with normal goat serum (5%) blocking solution for 30 minutes. Sections were incubated in primary xanthine oxidase antibody diluted at 1:50 in TBS for 60 minutes at 25°C. This was followed by two washes in PBS buffer for 2 minutes at 25°C. Secondary antibody incubation was done at a concentration of 1:40 (Rhodamine Red goat anti-rabbit IgG) for 60 min at 25°C in the dark. Final rinses in PBS-T (3x) at 2 minute intervals were performed on all sections. Slides were then mounted in fluorescent mounting medium with Dapi (Vector Laboratories) and images were acquired via a monochrome camera (Qimaging Retiga) attached to an inverted fluorescent microscope (Axiovert 200, Xeiss).

Myofiber Cross-Sectional Area. Sections from frozen diaphragm samples were cut at 10 microns using a cryotome (Shandon Inc., Pittsburgh, PA) and stained for dystrophin, myosin heavy chain (MHC) I and MHC type IIa proteins for fiber cross-sectional area analysis (CSA) as described previously (79). CSA was determined using Scion software (NIH).

Functional

Contractile Properties. Twitch characteristics and the force-frequency response of a strip of costal diaphragm were performed *in vitro* and normalized to cross-sectional area (CSA) as previously described (24, 98, 107).

Biochemical

Xanthine Dehydrogenase and Xanthine Oxidase Activities. The activities of XDH and XO were assayed using a fluorometric assay according to Beckman et al. (9). The principle of the assay involves the conversion of pterin into the fluorescent product isoxanthopterin. The rate of product formation with oxygen as the electron acceptor represents the activity of XO, whereas the combined activities of XO and XDH are measured with methylene blue as the electron acceptor. In brief, a section of the costal diaphragm was homogenized in a buffer containing 50 mM potassium phosphate, 0.1 mM EDTA, 0.25 M sucrose, and 0.2 mM PMSF (pH 7.4). The homogenates were centrifuged at 40,000 *g* for 30 min at 4°C. The supernatant was collected and assayed immediately. Briefly, XO activity was determined by the addition of 10 μM of pterin to 1 mg protein lysate while 10 μM of methylene blue was added to determine total XO + XDH activity. The conversion of pterin to the fluorescent product isoxanthopterin was monitored fluorometrically at an excitation of 345 nm and an emission of 390 nm at 37°C.

Hypoxanthine and Xanthine Levels. Hypoxanthine and xanthine were measured using the Amplex Red xanthine/xanthine oxidase assay kit from Invitrogen (Eugene, Oregon) as

described by the manufacturer and normalized to protein concentration. Briefly, a section of the costal diaphragm was homogenized 1:30 (wt/vol) in phosphate buffered saline (PBS). Samples were centrifuged at 3500 *g* for 30 min at 4°C. After collection of the resulting supernatant, diaphragmatic protein content was assessed by the method of Bradford (Sigma, St. Louis). Approximately fifty microliters of the supernatant was reacted with the assay cocktail solution for 30 min at 37°C in the dark. Absorbance was read at 560 nm. Hypoxanthine and xanthine standards were prepared and concentrations were calculated based on the standard curves.

Uric Acid Levels. Uric acid levels in the diaphragm were assessed using the uric acid assay kit from BioAssay Systems (Hayward, CA) as described by the manufacturer. Briefly, a section of the costal diaphragm was homogenized 1:30 (wt/vol) in phosphate buffered saline (PBS). Samples were centrifuged at 3500 *g* for 30 min at 4°C. After collection of the resulting supernatant, diaphragmatic protein content was assessed by the method of Bradford (Sigma, St. Louis). Approximately twenty microliters of the supernatant was reacted with the assay cocktail solution for 30 min at room temperature. Absorbance was read at 590 nm. A uric acid standard was prepared and concentrations were calculated based on this standard.

Western Blot Analysis. Protein content was determined in all samples via Western Blot analysis. Diaphragm samples were homogenized in a buffer containing 5 mM Tris (pH 7.5) and 5 mM EDTA (pH 8.0) with a protease inhibitor cocktail (Sigma, St. Louis). Homogenates were centrifuged at 1500 *g* for 10 min at 4°C. After centrifugation, the supernatant was collected and a protein assay (Bradford) was performed. Proteins from the supernatant fraction were separated via polyacrylamide gel electrophoresis, transferred to a nitrocellulose membrane, and incubated with primary antibodies directed against the protein of interest. 4-hydroxynonenal (4-HNE) was probed as a measurement indicative of oxidative stress while XOR was performed to visualize

both XDH and XO induction. Membranes were probed with Alexa Fluor 680 IgG secondary, scanned, and analyzed using the Odyssey system (Li-Cor Biosciences) using direct infrared fluorescent detection with a wide linear dynamic range.

Protein Carbonyls. Protein carbonyls were analyzed as an indicator of protein oxidation. Diaphragmatic protein carbonyls were measured in 40-50 mg total costal diaphragm muscle using a commercially available kit (Zenith Technology Corporation, Dunedin, NZ) according to the manufacturer's instructions.

Total Glutathione. Total glutathione content was measured as an indicator of nonenzymatic antioxidant status using a commercially available kit according to the manufacturer's instructions (Cayman Chemical, Ann Arbor, MI). Briefly, a section of the costal diaphragm was homogenized in 100 mM phosphate buffer containing 1 mM EDTA and 0.05% bovine serum albumin. Samples were centrifuged 10,000 *g* for 15 min at 4°C. The supernatant was deproteinated with an equal volume of metaphosphoric acid, centrifuged, and combined with 50 μl triethanolamine per milliliter of supernatant. Fifty microliters of deproteinated sample were reacted with the provided assay cocktail in the dark for 25 min. Absorbance was read at 405 nm. Standards were prepared using oxidized glutathione (GSSG), which is reduced to 2 mol equivalents of glutathione (GSH) under the assay conditions, and concentrations were calculated based on this standard curve.

Cell Culture Measurements

Trypan Blue Exclusion Assay. The trypan blue assay was used to assess cellular viability upon exposure to hydrogen peroxide (H_2O_2). Briefly, an aliquot of cell suspension was diluted 1:1 with 0.4% trypan blue and cells were counted with a hemocytometer. Results are

expressed as the percentage ratio of viable (unstained) cells in hydrogen peroxide treated samples vs. untreated samples.

Xanthine Dehydrogenase and Xanthine Oxidase Activities. The activities of XDH and XO were assayed using a fluorometric assay according to Beckman et al. (9).

Western Blot Analysis. Protein content was determined in all samples via Western Blot analysis. Myotubes were lysed in a buffer containing 30 mM Tris-HCL (pH 7.5), 250 mM Sucrose, 150 mM NaCl, 1 mM DTT, and protease inhibitor cocktail (Sigma, St. Louis). Lysates were centrifuged at 4°C for 10 minutes at 16000 g. After centrifugation, the supernatant was collected and a protein assay (Bradford) was performed. Proteins from the supernatant fraction were separated via polyacrylamide gel electrophoresis, transferred to a nitrocellulose membrane, and incubated with primary antibodies directed against the protein of interest. XOR was probed to visualize both XDH and XO induction during the experiments. Calpain activity was assessed by analyzing both total (non-active) and cleaved (active) calpain-1 and total (non-active) calpain-2. In addition, α-II spectrin was measured to obtain a more defined picture of calpain regulation with hydrogen peroxide treatment. Blots were imaged using an Odyssey system (Li-Cor Biosciences), using direct infrared fluorescent detection with a wide linear dynamic range.

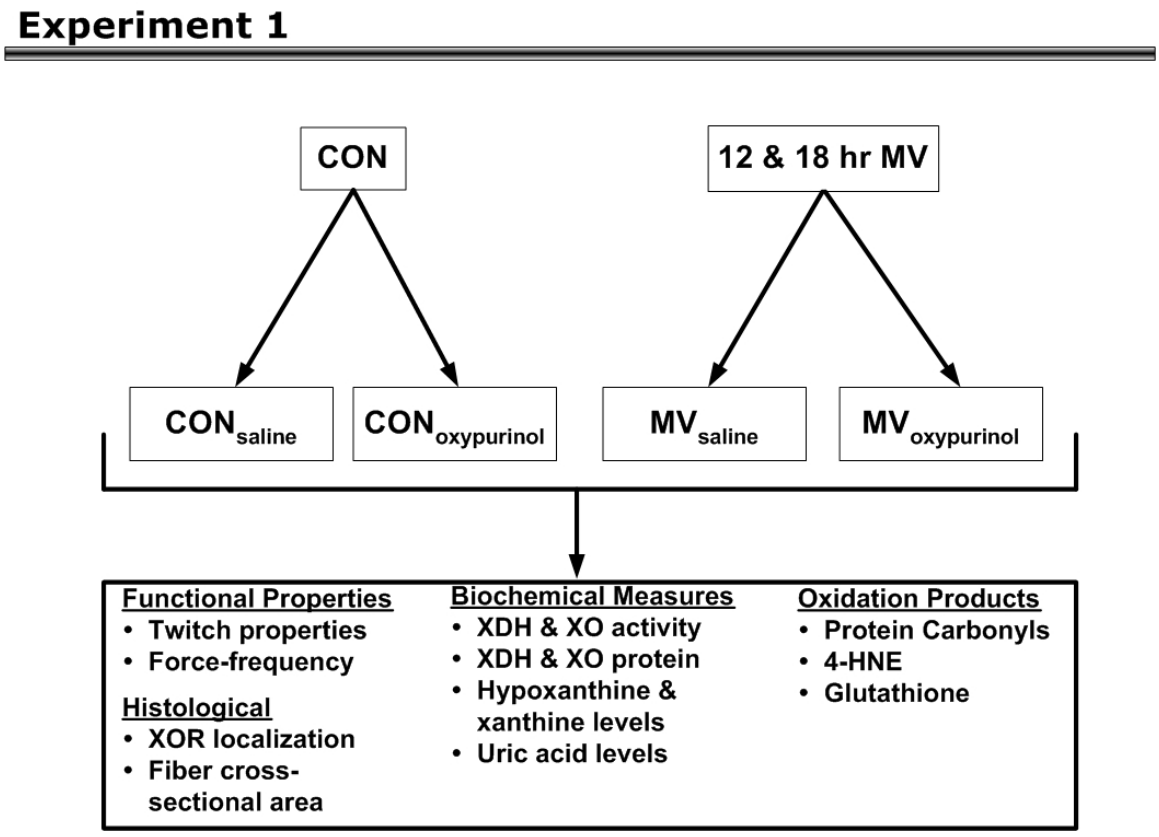

Figure 3-1. Experimental animal design used to determine if pharmacological inhibition of XO activity reduces MV-induced diaphragmatic oxidative stress and contractile dysfunction. Measurements from MV and MVOxypurinol were made vs. CON. We addressed Aim 1 by having two levels of MV at two different durations.

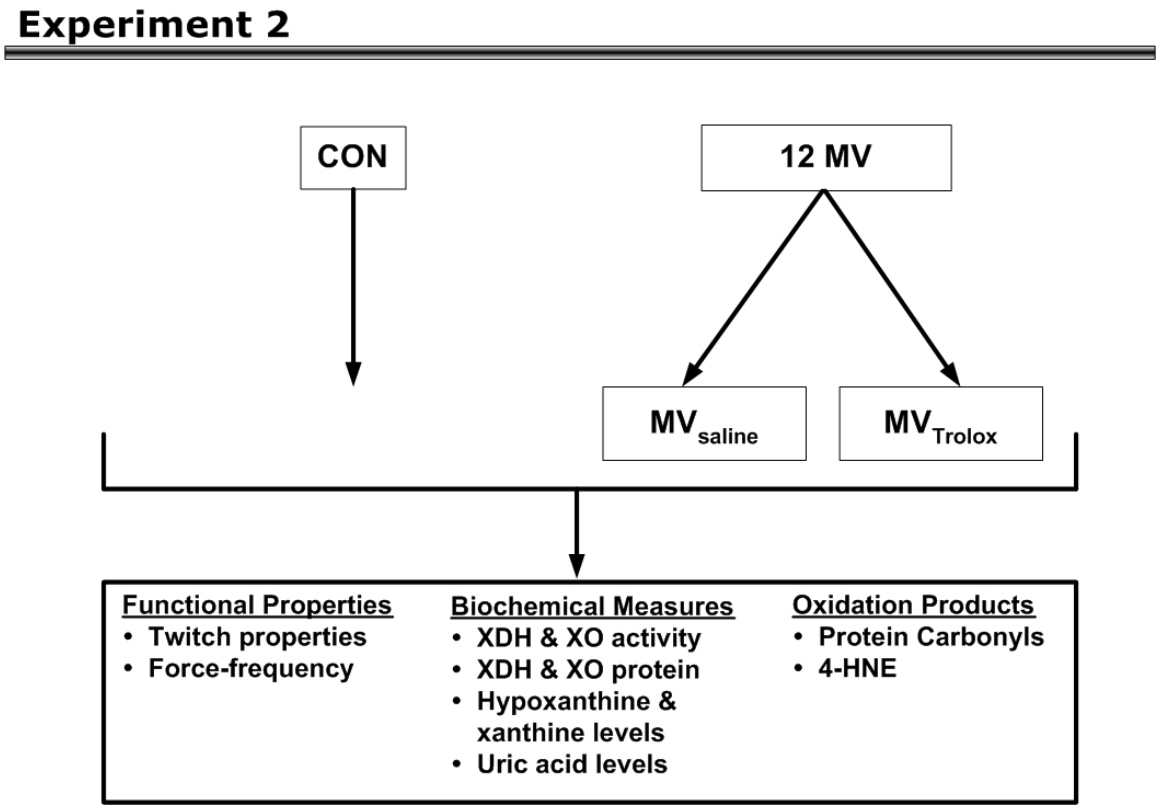

Figure 3-2. Experimental animal design used to examine whether the administration of an exogenous antioxidant during MV prevents XO activation in the diaphragm. Measurements from MV and MVTrolox were made vs. CON. We addressed Aim 2 by having two levels of MV.

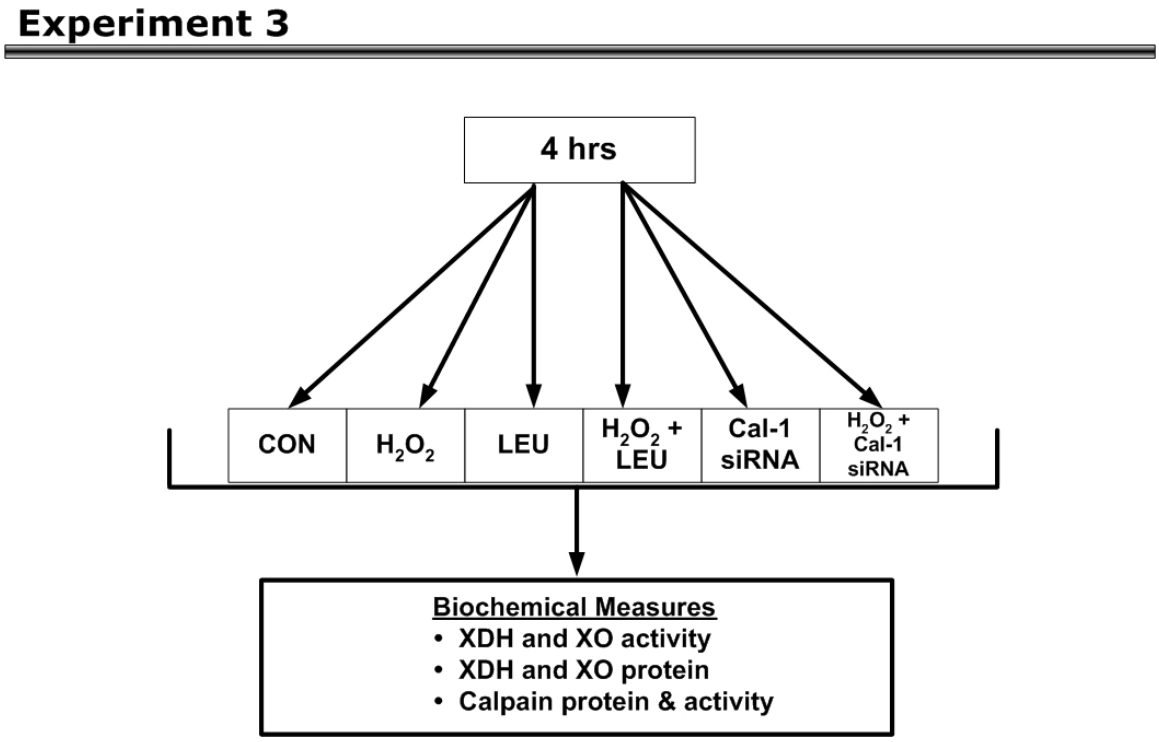

Figure 3-3. Experimental cell culture design used to determine if a ROS challenge activates XO in skeletal muscle myotubes. We addressed Aim 3 by using hydrogen peroxide to stimulate a ROS challenge to examine the reversible conversion of XDH to XO in skeletal muscle cells. In addition, leupetin and siRNA for calpain-1 were used in conjunction with hydrogen peroxide to ascertain whether calpain is the protease responsible for the irreversible conversion of XDH to XO in skeletal muscle cells.

CHAPTER 4
RESULTS

Experiment 1

Systemic Response to MV

To determine if the pharmacological inhibition of XO activity in the diaphragm reduces MV-induced oxidative stress and contractile dysfunction, we measured XOR protein and activity levels, key markers of oxidative stress, and contractile characteristics of our experimental animals. Animals used in experiment 1 were 4–6 months of age and weighed between 280-320 g before the experimental procedures. Neither the 12-hr or 18-hr MV protocols altered body weight ($P<0.05$). Heart rate (HR), systolic blood pressure (SBP), and body temperature (T) were maintained relatively constant during the MV protocols (HR range= 300–420 beats/min; SBP= 70–130 mmHg; T= 36-37°C). The arterial partial pressures of O_2 (PaO_2) and CO_2 ($PaCO_2$) were also maintained relatively constant during MV. Specifically, PaO_2 ranged from 65-100 mmHg whereas $PaCO_2$ ranged from 32-42 mmHg. In addition, at the completion of the MV protocol, there were no visual abnormalities of the lungs or peritoneal cavity, no evidence of lung infarction, and no evidence of infection, indicating that our aseptic surgical technique was successful.

XOR Characteristics

XOR Localization

Xanthine oxidoreductase (XOR) was been characterized in skeletal muscle of both humans and rats (40, 42). Figure 4-1 illustrates that XOR is primarily localized in the cytosol of rat diaphragm muscle. XOR, stained red, appears diffuse throughout the diaphragm muscle fibers as the nuclei, which are stained blue, are localized along the sarcolemma.

XDH and XO Activity Levels

Under normal conditions, mammalian XOR is synthesized as xanthine dehydrogenase (XDH). XDH uses NAD+ as its electron acceptor in the hydroxylation of hypoxanthine and xanthine to uric acid. To determine diaphragmatic levels of XDH activity, total XOR activity and XO activity were independently measured in our experimental groups. XDH activity was calculated by subtracting the level of XO activity from total XOR activity. Compared to control, 12 hours of MV resulted in a significant decrease in diaphragmatic XDH activity ($P<0.05$) (Table 4-1) and oxypurinol administration restored XDH activity to control values. Prolonged (18 hrs) MV tended to increase diaphragmatic XDH activity above control (Table 4-1), although this increase did not reach statistical significance. Nonetheless, 18 hours of MV resulted in a significant increase in total XOR activity (Table 4-1). Given that XDH activity is determined by the subtraction of XO activity from total XOR activity, as total activity increased in the diaphragm, so did XDH. Oxypurinol administration in the 18-hr MV animals resulted in a significant increase in both XDH and total XOR activities above control (Table 4-1). However, when XDH activity is expressed as a percent of total XOR activity, both MV durations resulted in a decrease in diaphragmatic XDH activity below control and XO inhibition restored XDH activity to control values.

In certain physiological conditions, XDH can be converted to XO. It is in this XO form that during the reduction of the purine substrates to uric acid, superoxide is produced. Compared to control, diaphragmatic XO activity significantly increased 25% and 43% in the MV animals at 12 and 18 hours, respectively ($P<0.05$) (Table 4-1). Oxypurinol administration significantly attenuated the increase in diaphragmatic XO activity back to control values. When XO activity is expressed as a percent of total XOR activity, MV resulted in a significant increase in

diaphragmatic XO activity. Furthermore, XO inhibition via oxypurinol administration significantly attenuated the MV-induced increase in diaphragmatic XO activity.

Since the level of superoxide production that occurs in skeletal muscle by the XO pathway is dependent upon the levels of XO to XDH in the muscle, we calculated the ratio of XO to XDH in our experimental groups. Compared to control, both 12 and 18 hours of MV resulted in a significant increase in XO/XDH activity in the diaphragm ($P<0.05$) (Figure 4-2). While oxypurinol administration in a group of control animals did not affect the ratio, it significantly attenuated the increase in XO to XDH activity in the diaphragms of our MV animals. Collectively, these results show that MV results in a significant increase in diaphragmatic XO activity and oxypurinol is an effective pharmacological agent to inhibit XO activity in the diaphragm during MV.

XDH and XO Protein Levels

To further understand the role of the XO pathway in oxidant production in the diaphragm during MV, we measured the protein level of XOR. XOR exists in two alternative forms that are derived from the same gene product (47). Initially, XOR is synthesized as a 150 kDa protein from which both XDH and XO are derived (130). Under normal conditions, XOR exists as XDH at a molecular weight of 150 kDa. However, XDH can be reversibly converted to XO via sulfhydryl oxidation which changes the enzymatic activity of XDH to XO but does not change its weight (101). Compared to control, only prolonged (18 hrs) MV resulted in a significant increase in the 150 kDa band of XOR in the diaphragm ($P<0.05$) (Figure 4-3). Moreover, compared to control, oxypurinol administration in both the 12 and 18 hr MV experimental groups resulted in a significant increase in the 150 kDa band of XOR in the diaphragm ($P<0.05$)

which was not observed in a group of oxypurinol-treated control animals. Thus, prolonged MV increases XOR protein (150 kDa) expression in the diaphragm.

Whereby both XDH and XO may exist in the diaphragm muscle as a 150 kDa band of XOR, only XO exists as a 130 kDa band of XOR. During activating conditions, XDH can be irreversibly converted to XO via proteolytic mechanisms. The proteolytic processing of XDH results in the cleavage of an approximately 15-20 kDa fragment, resulting in the formation of an active 130 kDa form of XO (22, 130). Compared to control, 12 and 18 hrs of MV resulted in a significant increase in the 130 kDa band of XOR in the diaphragm ($P<0.05$) (Figure 4-4). In addition, oxypurinol administration did not statistically alter XO protein levels in the diaphragms of either control or mechanically ventilated animals. Therefore, both MV durations resulted in a significant increase in the protein levels of XO (130 kDa) in the diaphragm and thus the irreversible proteolytic conversion of XDH to XO is significantly increased in the diaphragm during MV.

Enzyme Substrates and End Product

Hypoxanthine

Both XDH and XO catalyze the last two steps of purine catabolism resulting in the formation of uric acid from hypoxanthine and xanthine. Thus an increase in diaphragmatic XO activity would result in the depletion of purine substrates. Compared to control, MV resulted in a significant decrease in hypoxanthine levels in the diaphragm ($P<0.05$) (Figure 4-5). Twelve hours of MV resulted in an 11% decrease in hypoxanthine and 18 hours resulted in a 38% decrease. Oxypurinol administration failed to decrease hypoxanthine levels during prolonged (18 hrs) MV and there was only a trend ($P=0.09$) for oxypurinol to attenuate the decrease in hypoxanthine levels at 12 hours of MV. The depletion of hypoxanthine during MV coincides

with the MV-induced increase in diaphragmatic XO activity. Finally, XO inhibition did not significantly protect hypoxanthine levels during MV.

Xanthine

Similar to hypoxanthine, both MV durations resulted in a significant decrease in xanthine levels in the diaphragm ($P<0.01$) (Figure 4-6). Twelve hours of MV resulted in a 31% decrease in xanthine, whereas 18 hours resulted in a 41% decrease. XO inhibition via oxypurinol administration significantly attenuated the decrease in xanthine at both 12 and 18 hours of MV. Thus both MV durations resulted in a significant decrease in the level of purine substrates in the diaphragm. However, unlike hypoxanthine, oxypurinol administration significantly attenuated the MV-induced decrease in xanthine levels in the diaphragm.

Uric Acid

In the presence of the purine substrates and molecular oxygen, XO catalyzes the production of uric acid and superoxide. Accordingly, the level of uric acid formation in the diaphragm would increase in concomitant with an increase in diaphragmatic XO activity. Compared to control, 12 and 18 hrs of MV resulted in a significant 15% and 42% increase in uric acid formation in the diaphragm, respectively ($P<0.05$) (Figure 4-7). Although oxypurinol administration tended to attenuate the increase in uric acid at the 12 hour time point, it did not reach significance ($P=0.09$). In contrast, oxypurinol administration significantly attenuated the formation of uric acid in the diaphragms of our 18-hr MV animals. Thus MV results in a significant increase in uric acid, an end product of both XDH and XO enzymatic activity, in the diaphragm. This coincides with the MV-induced increase in diaphragmatic XO activity and depletion of the purine substrates in the diaphragm.

Redox Balance

Protein Carbonyls

Since MV results in an increase in diaphragmatic XO activity, the potential for ROS production by the XO pathway exists in the diaphragm. Protein carbonyl formation is a general indicator of protein oxidation and commonly used to measure oxidative injury. Twelve hours of MV resulted in a significant increase in protein carbonyl formation in the diaphragm when compared with control ($P<0.05$) (Figure 4-8) and there was a trend ($P=0.07$) for oxypurinol administration to attenuate this increase. Prolonged (18 hrs) MV further elevated the levels of protein carbonyl formation in the diaphragm when compared with 12 hrs of MV ($P<0.05$). While oxypurinol administration significantly attenuated the increase in protein carbonyls at the 18-hr time point, protein carbonyl formation in the diaphragm remained significantly elevated when compared with control. Thus, XO inhibition attenuates some of the MV-induced protein oxidation in the diaphragm

4-HNE

Lipid peroxidation occurs as a response to oxidative stress, and among the end-products it produces several biologically active aldehydes. 4-hydroxynoneal (4-HNE) is an unsaturated α,β hydroxyalkenal that is generated during the lipid peroxidation cascade. Furthermore, 4-HNE is the primary adduct formed during this process and is commonly used to assess protein oxidative damage. Compared to control, both MV durations resulted in a significant increase in diaphragmatic 4-HNE ($P<0.05$) (Figure 4-9). XO inhibition significantly attenuated the accumulation of 4-HNE as oxypurinol treated animals had basal levels of diaphragmatic 4-HNE. Therefore, diaphragmatic XO activity contributes to MV-induced oxidative stress by the fact that

XO inhibition reduces protein oxidation and significantly attenuates lipid peroxidation in the diaphragm.

Total Glutathione

Glutathione (GSH) is the major nonezymatic antioxidant component of the cell and depletion of cellular stores is generally considered indicative of oxidative stress. Following 12 and 18 hours of MV, there was a significant depletion of total GSH in the diaphragm ($P<0.05$) (Figure 4-10) and oxypurinol administration failed to attenuate this decrease. Consequently, MV results in the depletion of the antioxidant defense of the diaphragm and XO inhibition does not rescue this depletion.

Contractile Function

Maximal Isometric Twitch Force

To determine if XO-mediated ROS production in the diaphragm contributes to diaphragmatic contractile dysfunction, we measured maximal isometric twitch force and analyzed the force-frequency response of diaphragm strips obtained from our experimental animals. Maximal isometric twitch forces of *in vitro* costal diaphragm strips from mechanically ventilated and nonmechanically ventilated (control) animals with and without oxypurinol are presented in Table 4-2. Maximal isometric twitch force was significantly reduced following 18 hrs of MV when compared with control and control with oxypurinol. During prolonged (18 hrs) MV, there was a trend ($P=0.07$) for XO inhibition via oxypurinol administration to attenuate the drop in maximal isometric twitch force. Accordingly, prolonged MV results in a significant decrease in maximal isometric twitch force of the diaphragm and oxypurinol administration during MV appears to restore some of this decrease.

Force-Frequency Response

Mean maximal force-frequency responses of *in vitro* costal diaphragm strips from mechanically ventilated and nonmechanically ventilated (control) animals with and without oxypurinol are presented in Figure 4-11. Both 12 and 18 hours of MV shifted the force-frequency response down when compared with control (CON) and control animals treated with oxypurinol (CONO). Twelve and eighteen hours of MV resulted in a significant reduction in the specific force of the diaphragm compared to the control groups at all stimulation frequencies. Specifically, both MV durations resulted in a 23% decrease in maximal diaphragmatic specific force. Treatment with oxypurinol prior to MV (12MVO and 18MVO) attenuated the MV-induced diaphragmatic dysfunction at stimulation frequencies above 60 hertz. So XO inhibition attenuated some of the MV-induced contractile dysfunction that is normally observed.

Diaphragmatic Atrophy

Cross-sectional Area

To evaluate the impact of XO inhibition on MV-induced diaphragmatic atrophy, we compared the cross-sectional areas (CSA) of diaphragmatic myofibers across our experimental groups. Compared to control, we observed a significant decrease ($P<0.05$) in diaphragmatic type I fiber CSA following 12 and 18 hours of MV (Figure 4-12). While oxypurinol administration at both MV time points appears to attenuate the decrease in type I myofiber cross-sectional area, it did not reach statistical significance ($P=0.1$). Diaphragmatic type IIa fiber CSA followed the same pattern as the type I fibers, whereby both 12 and 18 hours of MV resulted in a significant reduction in type IIa fiber CSA in the diaphragm ($P<0.05$) (Figure 4-13). There was a trend ($P=0.07$) for oxypurinol administration to attenuate the decrease in type IIa CSA following 12 hours of MV. Finally, significant decreases in CSA for type IIb/x fibers were observed in

diaphragms from both MV groups (Figure 4-14) although no significant differences existed in fiber CSA between control and oxypurinol treated MV animals. Therefore, while XO contributes to both MV-induced oxidative stress and contractile dysfunction, XO inhibition does not appear to attenuate diaphragmatic atrophy during MV.

Experiment 2

Systemic Response to MV

To ascertain whether the administration of an exogenous antioxidant during MV prevents diaphragmatic XO activation, we administered Trolox to a subset of MV animals and measured oxidative stress, contractile function, and XOR protein and activity levels in the diaphragms of our experimental animals in experiment 2. All of the animals were 4–6 months of age. No significant differences existed in body weight between the groups (CON = 0.305 g ± 0.005, 12MV = 0.294 g ± 0.003, and 12MVT = 0.298 g ± 0.004) before the experiment, and the 12-hr experimental protocol did not alter body weight ($P<0.05$). Heart rate (HR), systolic blood pressure (SBP), and body temperature (T) were maintained within a normal physiological range during the MV protocol (HR range= 300–420 beats/min; SBP= 70–130 mmHg; T= 36-37°C). The arterial partial pressures of O_2 (PaO_2) and CO_2 ($PaCO_2$) were also maintained relatively constant during MV. Specifically, PaO_2 ranged from 60-89 mmHg whereas $PaCO_2$ ranged from 34-46 mmHg. In addition, at the completion of the MV protocol, there were no visual abnormalities of the lungs or peritoneal cavity, no evidence of lung infarction, and no evidence of infection, indicating that our aseptic surgical technique was successful.

Redox Balance

Protein Carbonyls

In experiment 1, we demonstrated that the irreversible proteolytic conversion of XDH to XO is increased in the diaphragm during MV to induce XO activity. This proteolytic conversion

is thought to occur subsequent to the reversible conversion of XDH to XO via sulfhydryl oxidation of cysteine residues (14, 83). To ascertain whether the reversible conversion via oxidation is a required step by which diaphragmatic XO activity is increased during MV, we used Trolox to attenuate the oxidative stress that occurs during ventilation. By attenuating the MV-induced diaphragmatic oxidative stress, we theorized that any sulfhydrl oxidation of cysteine residues on XDH would be eliminated. To demonstrate the effectiveness of Trolox as an appropriate pharmacological agent to restore diaphragmatic redox balance, protein carbonyl formation and 4-HNE levels were measured. Twelve hours of MV resulted in a significant increase in protein carbonyl formation in the diaphragm ($P<0.05$) when compared with control (Figure 4-15). More importantly, Trolox administration significantly attenuated the increase in protein carbonyls in the diaphragm.

4-HNE

Compared to control, 12 hours of MV resulted in a significant increase in diaphragmatic 4-HNE ($P<0.05$) (Figure 4-16). Trolox administration significantly attenuated the accumulation of 4-HNE as Trolox treated animals had basal levels of diaphragmatic 4-HNE. Thus we have shown that Trolox administration during MV effectively inhibits diaphragmatic oxidative stress by the complete attenuation of protein oxidation and lipid peroxidation in the diaphragm of Trolox-treated MV animals.

Contractile Function

Maximal Isometric Twitch Force

Maximal isometric twitch force and force-frequency responses were measured in our experimental groups to further demonstrate the effectiveness of Trolox in maintaining redox balance. Maximal isometric twitch forces of *in vitro* costal diaphragm strips from control,

mechanically ventilated, and mechanically ventilated animals with Trolox are presented in Table 4-3. Maximal isometric twitch force was significantly reduced 30% following 12 hrs of MV when compared with controls ($P<0.05$) and Trolox administration significantly attenuated the drop in diaphragmatic maximal isometric twitch force.

Force-Frequency Response

The mean maximal force-frequency responses of *in vitro* costal diaphragm strips from control, mechanically ventilated, and mechanically ventilated animals with Trolox are presented in Figure 4-17. Twelve hours of MV shifted the force-frequency response down when compared with control. In fact, 12 hours of MV resulted in a significant reduction ($P<0.05$) in the specific force of the diaphragm compared to the control group at all stimulation frequencies. Treatment with Trolox during MV significantly attenuated the MV-induced diaphragmatic contractile dysfunction at all stimulation frequencies. Therefore, Trolox administration is a potentially useful therapeutic approach to attenuate MV-induced diaphragmatic contractile dysfunction.

XOR Characteristics

XDH and XO Activity Levels

To examine the reversible conversion of XDH to XO in the diaphragm during MV, we measured total XOR, XDH, and XO activities in the diaphragms of our control, mechanically ventilated, and mechanically ventilated animals with Trolox. If the reversible conversion of XDH to XO is present in the diaphragm during MV, then we would expect to find an increase in diaphragmatic XDH activity along with a concomitant decrease in XO activity in our Trolox-treated MV animals when compared with our regular MV animals. Compared to control, MV resulted in a significant decrease in diaphragmatic XDH activity ($P<0.05$) (Figure 4-18) along with an increase in XO activity ($P<0.05$) (Figure 4-19). Trolox administration failed to attenuate the changes in both XDH and XO activity in the diaphragm. Because Trolox administration

during MV did not attenuate diaphragmatic XO activity, it appears that the reversible conversion of XDH to XO via oxidation does not occur in the diaphragm during MV when oxidative stress in prevented with Trolox.

XDH and XO Protein Levels

Because the reversible conversion only changes enzymatic activity and not molecular weight, Trolox administration during MV should not alter the protein expression of the 150 kDa band of XOR or directly change the 130 kDa band produced via the irreversible proteolytic process. No significant differences existed in the 150 kDa band of XOR (Figure 4-20) in the diaphragm between our experimental groups. In addition, Trolox administration did not attenuate the MV-induced induction of the 130 kDa band of XOR in the diaphragm ($P<0.05$) (Figure 4-21).

Enzyme Substrates and End Product

Given that Trolox administration during MV failed to alter diaphragmatic XO activity, purine substrate and uric acid levels would not be expected to change in our MV animals treated with Trolox. The levels of hypoxanthine, xanthine, and uric acid for control, mechanically ventilated, and mechanically ventilated animals with Trolox are presented in Table 4-4. Compared to control, 12 hours of MV resulted in a significant decrease in both hypoxanthine (~16%) and xanthine (~19%) in the diaphragm ($P<0.05$) and Trolox administration did not rescue these levels. With regards to uric acid, compared to control, 12 hours of MV resulted in a significant 17% increase in uric acid formation in the diaphragm ($P<0.05$). Again, Trolox administration failed to attenuate this increase in the diaphragm during MV. The fact that Trolox administration failed to alter the MV-induced changes in the levels of diaphragmatic hypoxanthine, xanthine, and uric acid, further demonstrate that the reversible conversion of XDH

to XO via oxidation does not occur in the diaphragm during MV when redox balance is maintained with Trolox.

Experiment 3

Myogenic Cells

Cell Viability

To determine if a ROS challenge activates XO in skeletal muscle myotubes, we used the C_2C_{12} myogenic cell line in our third experiment. We performed cell viability measurements on C_2C_{12} myotubes treated with and without hydrogen peroxide (100 μM) for 4 hours. These measurements were performed to determine if the hydrogen peroxide treatment was toxic to our cell line. Importantly, our results revealed that hydrogen peroxide treatment was not toxic to myocytes in our experimental model as indicated by the failure of myotubes to take up Trypan blue (97% viable).

XDH and XO Activity Levels

To investigate the mechanism(s) responsible for XO activation, we utilized a myogenic cell line to determine the effect of a ROS challenge (H_2O_2) on XO activation in skeletal muscle myotubes. Both XDH and XO activities were assessed in our cultured myotubes to determine if there was a similar increase in XO activity in cell culture compared to the *in vivo* animal experiments. In doing so, we examined the irreversible conversion of XDH to XO in skeletal muscle cells. Hydrogen peroxide was used to mediate the oxidation of the cysteine residues on XDH and both leupeptin and short interference RNA (siRNA) for calpain-1 were used to inhibit the activity of calpain which is up-regulated with hydrogen peroxide treatment. Calpain was examined as the protease responsible for the irreversible proteolytic processing of XDH to XO.

There were no significant differences in XDH activity in our experimental cell groups treated with or without hydrogen peroxide (Figure 4-22). However, there was a 21% increase in XO activity in cells treated with hydrogen peroxide ($P<0.05$) (Figure 4-23). Moreover, siRNA for calpain-1 failed to attenuate the hydrogen peroxide-induced increase in XO activity in skeletal muscle myotubes. However, hydrogen peroxide-induced XO activation was significantly attenuated with leupeptin. So while it appears that hydrogen peroxide induction of XO activity in C_2C_{12}s involves calpain activity or another protease inhibited by leupeptin, it appears that calpain-1 is not involved in the increase in XO activity in skeletal muscle myotubes with a hydrogen peroxide challenge.

XDH and XO Protein Levels

Measurements were also made to assess XOR protein content in our cultured myotubes to determine if there was a similar induction of XOR in cell culture compared to the *in vivo* animal experiments. There were no significant differences between our cell treatment groups in the protein expression of the 150 kDa band of XOR (Figure 4-24). However, when compared to control, hydrogen peroxide treated cells exhibited an approximate 1.4 fold increase in the 130 kDa band of XOR (Figure 4-25). The increase in the 130 kDa band of XOR was also observed in cells treated with both hydrogen peroxide and siRNA for calpain-1, although not when cells were treated with hydrogen peroxide and leupeptin or when cells were treated with leupeptin or siRNA for calpain-1 alone. The observation that compared to hydrogen peroxide treatment alone, cells treated with hydrogen peroxide and siRNA for calpain-1 exhibited the same significant increase in the 130 kDa band of XOR and cells treated with hydrogen peroxide and leupeptin prevented the induction of the 130 kDa band, suggests that a calpain protease is involved in XO activation in skeletal muscle myotubes but specifically eliminates calpain-1 as

the protease responsible for the irreversible proteolytic conversion of XDH to XO in skeletal muscle cells.

Calpain Protein and Activity

To demonstrate the effectiveness of both leupeptin and siRNA to inhibit calpain activity, measurements for calpain protein abundance and activity were made in our experimental cell groups. Compared to control, leupeptin treated cells exhibited a significant reduction in total calpain-1 protein (Figure 4-26). There was a trend for both siRNA for calpain-1 (P=0.08) and hydrogen peroxide plus siRNA for calpain-1 (P=0.06) to reduce total calpain-1 protein expression in skeletal muscle myotubes. As expected, compared to control, cells treated with hydrogen peroxide resulted in a significant increase in the cleaved or active band of calpain-1 (Figure 4-27). However, cells treated with either leupeptin or siRNA for calpain-1 resulted in a significant reduction in cleaved calpain-1. Furthermore, cleaved calpain-1 remained depressed below control values when cells where treated with both hydrogen peroxide and either inhibitor. Finally, there were no significant differences between our cell treatment groups in the protein expression of total calpain-2 (Figure 4-28).

Lastly, to further demonstrate the effectiveness of our calpain inhibitors, the calpain specific degradation product of α-II spectrin was measured. The intact form of α-II spectrin exists as ~250 kDa protein and upon degradation yields a 145 kDa (calpain-specific) cleaved band. Thus, *in vivo* calpain activity can be determined by probing for the calpain-specific α-II spectrin cleaved degradation product. There were no significant differences between our cell treatment groups in the protein expression of total α-II spectrin (Figure 4-29). Compared to control, cells treated with hydrogen peroxide resulted in a significant 1.5 fold induction of the calpain-specific cleaved α-II spectrin band (145 kDa) (Figure 4-30). On the other hand, there

were no increases in the calpain-specific cleaved α-II spectrin degradation product when cells were treated with either leupeptin, hydrogen peroxide and leupeptin, siRNA for calpain-1, or hydrogen peroxide and siRNA for calpain-1. Thus, leupeptin and siRNA for calpain-1 were completely effective in preventing the increase in calpain activity observed with hydrogen peroxide treatment.

Table 4-1. Total xanthine oxidoreductase (XOR), xanthine dehydrogenase (XDH), and xanthine oxidase (XO) activities in diaphragm from control, mechanically ventilated, and mechanically ventilated animals with oxypurinol.

Activity (μmol/min/g)	CON	CONO	12MV	12MVO	18MV	18MVO
Total XOR	0.131 ± 0.004	0.148 ± 0.004	0.126 ± 0.004	0.126 ± 0.004	0.165 ± 0.007$^{*\Psi\blacklozenge}$	0.183 ± 0.008$^{*\#\Psi\blacklozenge}$
XDH	0.075 ± 0.006 (57%)	0.088 ± 0.010 (59%)	0.056 ± 0.003$^{*\#}$ (44%)	0.078 ± 0.002 (62%)	0.085 ± 0.008 (52%)	0.126 ± 0.013$^{*\#\Psi\blacklozenge\Delta}$ (69%)
XO	0.056 ± 0.003 (43%)	0.060 ± 0.005 (41%)	0.070 ± 0.003* (56%)	0.048 ± 0.005$^{\Psi}$ (38%)	0.080 ± 0.005$^{*\#\blacklozenge}$ (48%)	0.057 ± 0.006$^{\Delta}$ (31%)

Values are expressed as mean ± SE. The values in parentheses represent the percent activity of total XOR activity. *Significantly different versus CON ($P<0.05$). $^{\#}$Significantly different from CONO ($P<0.05$). $^{\Psi}$Significantly different from 12MV ($P<0.05$). $^{\blacklozenge}$Significantly different from 12MVO. $^{\Delta}$Significantly different from 18MV ($P<0.05$). CON= Control; CONO= Control with oxypurinol; 12MV= 12 hrs mechanical ventilation; 12MVO= 12MV with oxypurinol; 18MV= 18 hrs mechanical ventilation; 18MVO= 18MV with oxypurinol.

Table 4-2. Maximal isometric twitch force production in diaphragm strips obtained from mechanically ventilated and nonmechanically ventilated (control) animals with and without oxypurinol.

Experimental Group	Maximal Isometric Twitch Force, N/cm^2
Control	10.1 ± 0.3
Control with oxypurinol	10.1 ± 0.1
18 h of MV	6.3 ± 0.4$^{*\#}$
18 h of MV with oxypurinol	8.2 ± 0.8

Values are expressed as mean ± SE. *Significantly decreased versus Control ($P<0.001$). $^{\#}$Significantly decreased versus Control with oxypurinol ($P<0.001$).

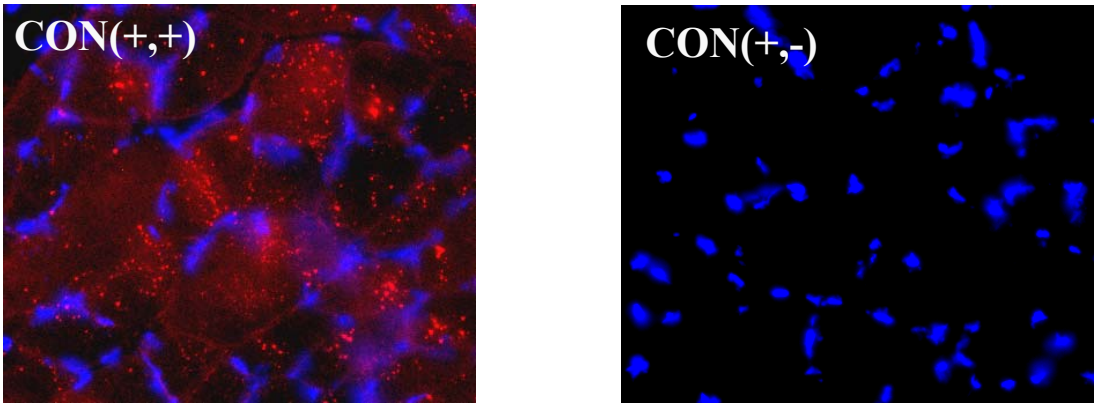

Figure 4-1. Xanthine oxidoreductase (XOR) localization in a control diaphragm muscle sample. XOR appears to be localized in the cytosol. Red stain= XOR and blue stain= nuclei. (+,+); Both primary and secondary antibody application; (+,-); Primary antibody application alone.

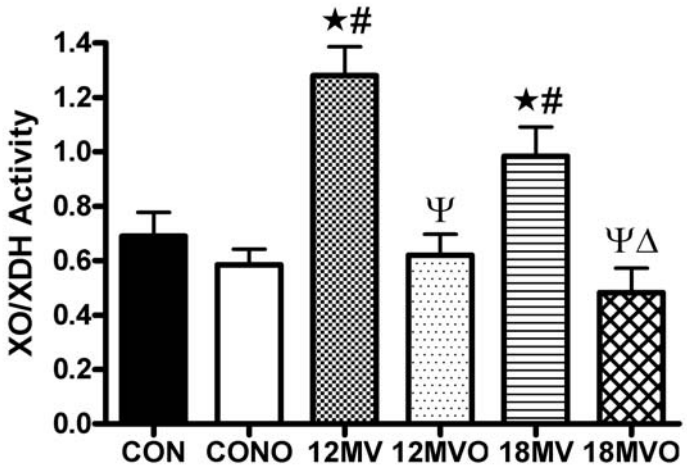

Figure 4-2. Ratio of xanthine oxidase (XO) activity to xanthine dehydrogenase (XDH) activity in diaphragm samples from experiment 1. Values are mean fold change ± SE. *Significantly increased versus CON ($P<0.05$). $^{\#}$Significantly increased versus CONO ($P<0.05$). $^{\Psi}$Significantly decreased versus 12MV ($P<0.001$). $^{\Delta}$Significantly decreased versus 18MV ($P<0.01$). CON= Control; CONO= Control with oxypurinol; 12MV= 12 hrs mechanical ventilation; 12MVO= 12MV with oxypurinol; 18MV= 18 hrs mechanical ventilation; 18MVO= 18MV with oxypurinol.

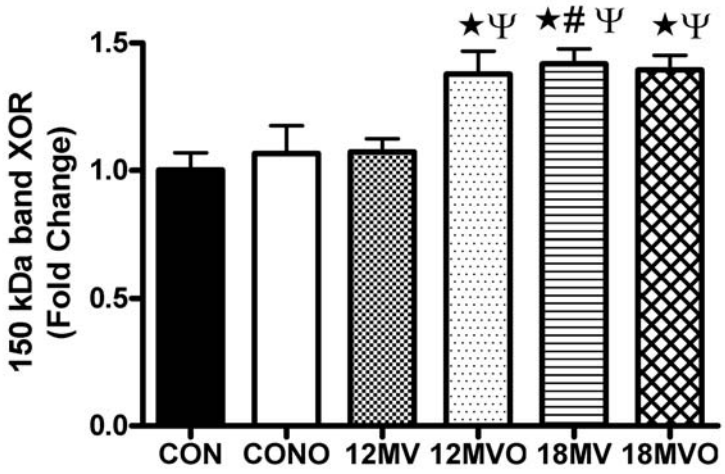

Figure 4-3. Fold changes (versus control) of XOR protein (150 kDa band) content in diaphragm samples from experiment 1. Values are mean fold change ± SE. *Significantly increased versus CON (P<0.01). #Significantly increased versus CONO (P<0.05). ΨSignificantly increased versus 12MV (P<0.05). CON= Control; CONO= Control with oxypurinol; 12MV= 12 hrs mechanical ventilation; 12MVO= 12MV with oxypurinol; 18MV= 18 hrs mechanical ventilation; 18MVO= 18MV with oxypurinol.

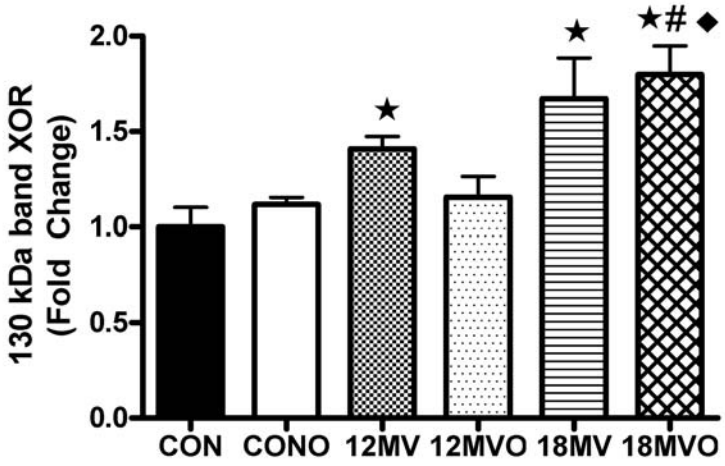

Figure 4-4. Fold changes (versus control) of XOR protein (130 kDa) content in diaphragm samples from experiment 1. Values are mean fold change ± SE. *Significantly increased versus CON (P<0.05). #Significantly increased versus CONO (P<0.05). ♦Significantly increased versus 12MVO (P<0.05). CON= Control; CONO= Control with oxypurinol; 12MV= 12 hrs mechanical ventilation; 12MVO= 12MV with oxypurinol; 18MV= 18 hrs mechanical ventilation; 18MVO= 18MV with oxypurinol.

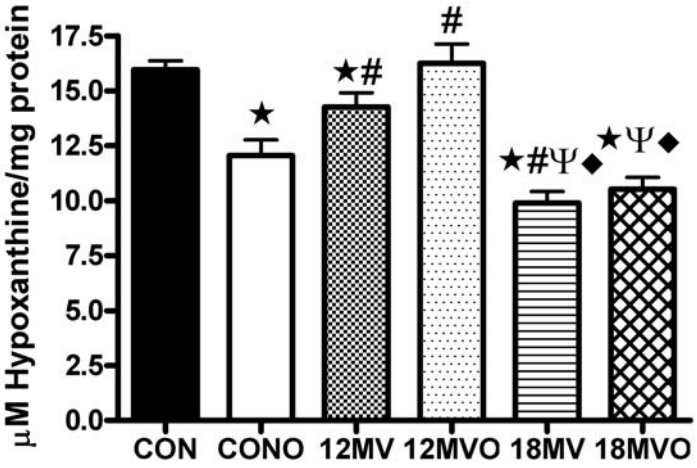

Figure 4-5. Hypoxanthine levels in diaphragm samples from experiment 1. Values are mean ± SE. *Significantly decreased versus CON (P<0.05). #Significantly different versus CONO (P<0.05). ΨSignificantly decreased versus 12MV (P<0.01). ♦Significantly decreased versus 12MVO (P<0.001). CON= Control; CONO= Control with oxypurinol; 12MV= 12 hrs mechanical ventilation; 12MVO= 12MV with oxypurinol; 18MV= 18 hrs mechanical ventilation; 18MVO= 18MV with oxypurinol.

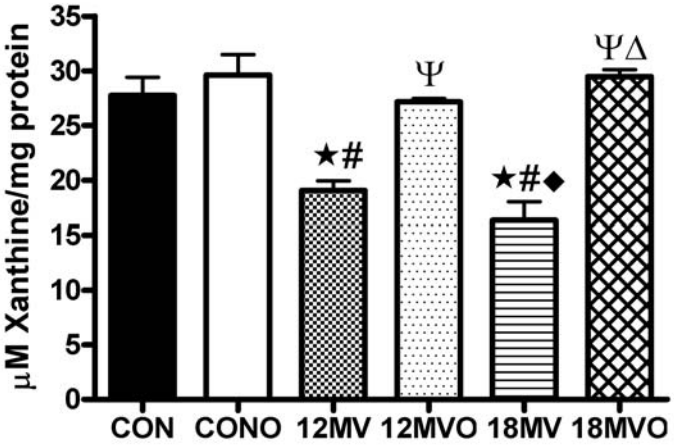

Figure 4-6. Xanthine levels in diaphragm samples from experiment 1. Values are mean ± SE. *Significantly decreased versus CON (P<0.01). #Significantly decreased versus CONO (P<0.001). ΨSignificantly increased versus 12MV (P<0.01). ♦Significantly decreased versus 12MVO (P<0.001). ΔSignificantly increased versus 18MV (P<0.001). CON= Control; CONO= Control with oxypurinol; 12MV= 12 hrs mechanical ventilation; 12MVO= 12MV with oxypurinol; 18MV= 18 hrs mechanical ventilation; 18MVO= 18MV with oxypurinol.

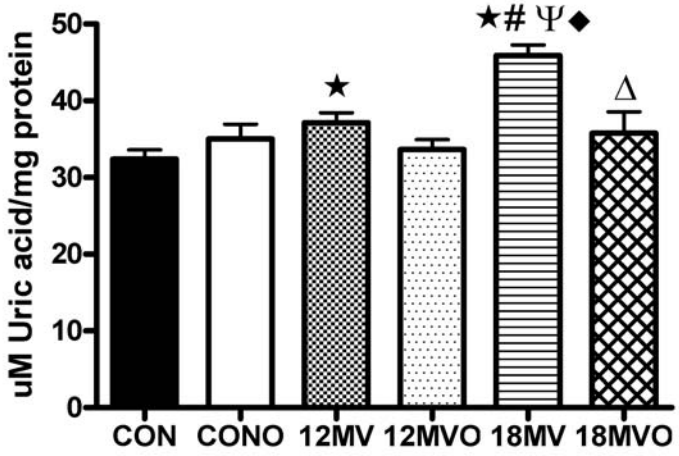

Figure 4-7. Uric acid levels in diaphragm samples from experiment 1. Values are mean ± SE. *Significantly increased versus CON (P<0.05). #Significantly increased versus CONO (P<0.01). ΨSignificantly increased versus 12MV (P<0.05). ♦Significantly increased versus 12MVO (P<0.01). ΔSignificantly decreased versus 18MV (P<0.01). CON= Control; CONO= Control with oxypurinol; 12MV= 12 hrs mechanical ventilation; 12MVO= 12MV with oxypurinol; 18MV= 18 hrs mechanical ventilation; 18MVO= 18MV with oxypurinol.

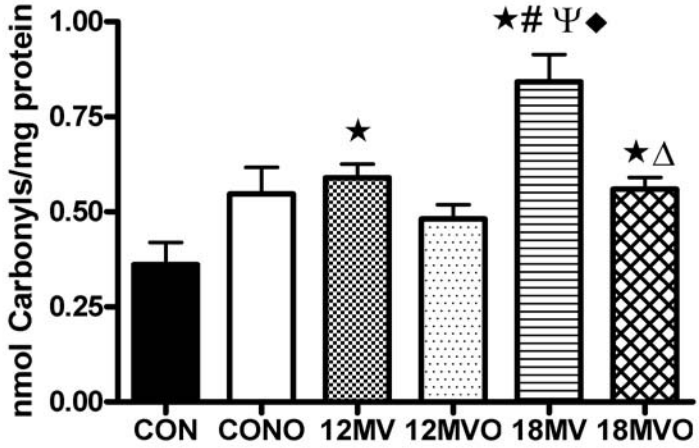

Figure 4-8. Protein carbonyl levels in diaphragm samples from experiment 1. Values are mean ± SE. *Significantly increased versus CON (P<0.05). #Significantly increased versus CONO (P<0.05). ΨSignificantly increased versus 12MV (P<0.05). ♦Significantly increased versus 12MVO (P<0.01). ΔSignificantly decreased versus 18MV (P<0.05). CON= Control; CONO= Control with oxypurinol; 12MV= 12 hrs mechanical ventilation; 12MVO= 12MV with oxypurinol; 18MV= 18 hrs mechanical ventilation; 18MVO= 18MV with oxypurinol.

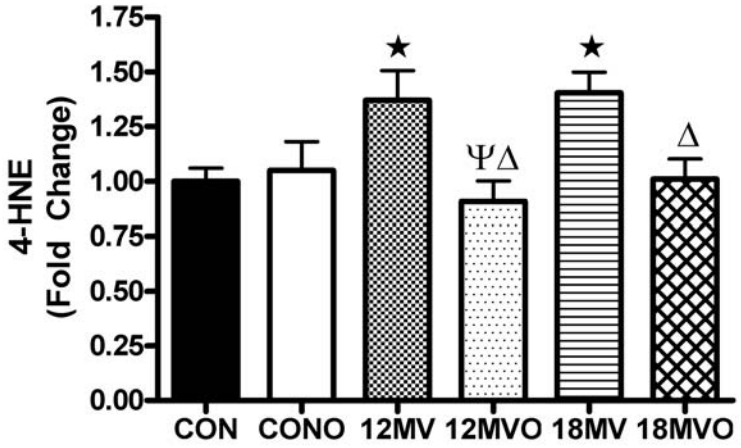

Figure 4-9. Fold changes (versus control) of 4-hydroxynonenal (4-HNE) accumulation in diaphragm samples from experiment 1. Values are mean fold change ± SE. *Significantly increased versus CON (P<0.05). Ψ Significantly decreased versus 12MV (P<0.05). Δ Significantly decreased versus 18MV (P<0.05). CON= Control; CONO= Control with oxypurinol; 12MV= 12 hrs mechanical ventilation; 12MVO= 12MV with oxypurinol; 18MV= 18 hrs mechanical ventilation; 18MVO= 18MV with oxypurinol.

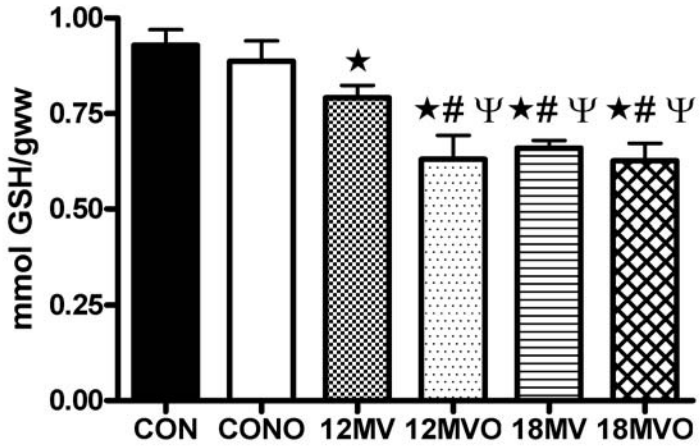

Figure 4-10. Total glutathione concentrations in diaphragm samples from experiment 1. Values are mean ± SE. *Significantly decreased versus CON (P<0.05). # Significantly decreased versus CONO (P<0.01). Ψ Significantly decreased versus 12MV (P<0.05). CON= Control; CONO= Control with oxypurinol; 12MV= 12 hrs mechanical ventilation; 12MVO= 12MV with oxypurinol; 18MV= 18 hrs mechanical ventilation; 18MVO= 18MV with oxypurinol.

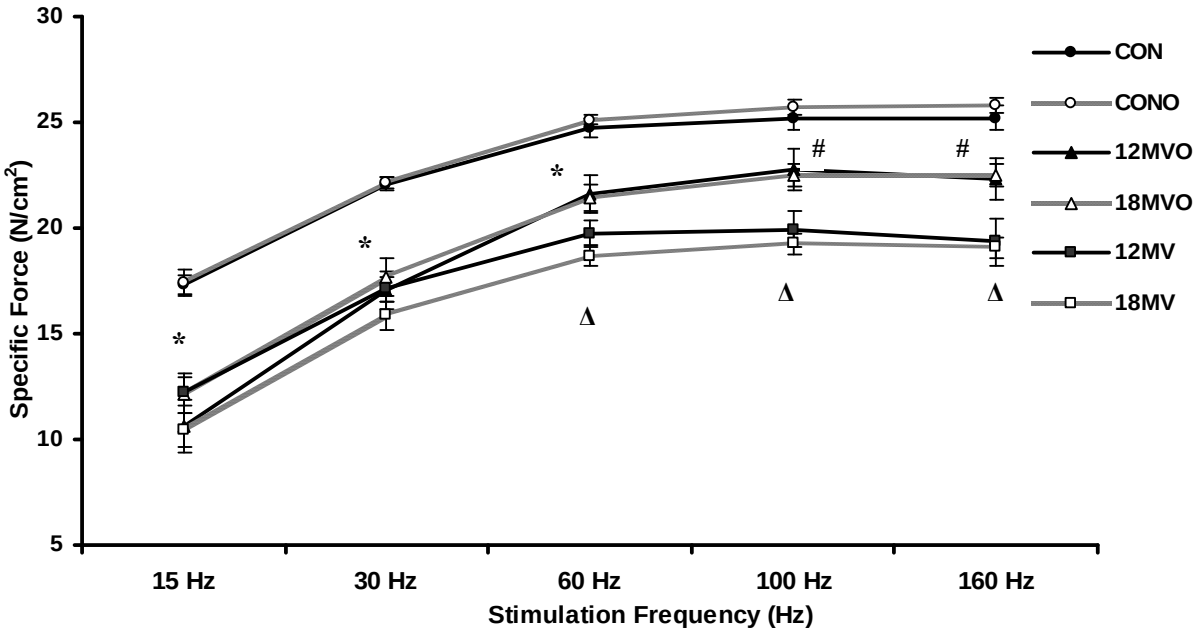

Figure 4-11. Diaphragmatic force-frequency response (*in vitro*) of diaphragm samples from experiment 1. Values are expressed as mean ± SE. *12MV, 18MV, 12MVO, and 18MVO significantly decreased versus CON and CONO (P<0.01). #Significantly decreased versus CON and CONO, except 12MVO and 18MVO (P<0.05). Δ18MV significantly decreased versus 12MVO and 18MVO (P<0.05). CON= Control; CONO= Control with oxypurinol; 12MV= 12 hrs mechanical ventilation; 12MVO= 12MV with oxypurinol; 18MV= 18 hrs mechanical ventilation; 18MVO= 18MV with oxypurinol.

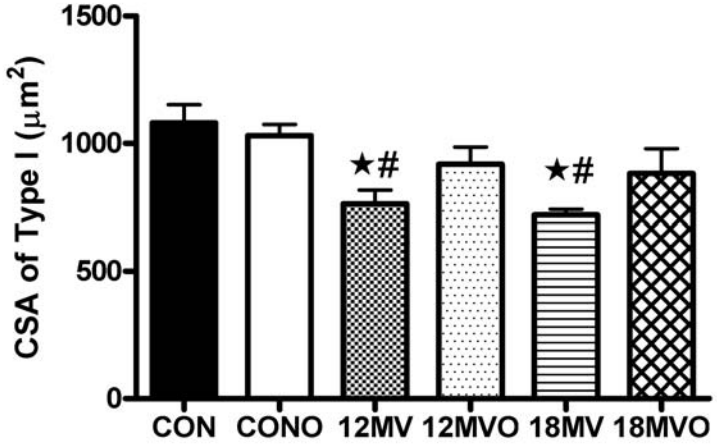

Figure 4-12. Type I fiber cross-sectional area in diaphragm samples from experiment 1. Values are mean ± SE. *Significantly decreased versus CON (P<0.05). #Significantly decreased versus CONO (P<0.05). CON= Control; CONO= Control with oxypurinol; 12MV= 12 hrs mechanical ventilation; 12MVO= 12MV with oxypurinol; 18MV= 18 hrs mechanical ventilation; 18MVO= 18MV with oxypurinol.

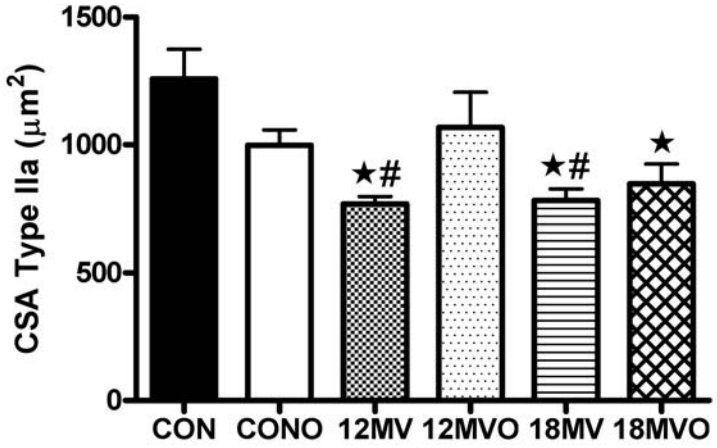

Figure 4-13. Type IIa fiber cross-sectional area in diaphragm samples from experiment 1. Values are mean ± SE. *Significantly decreased versus CON (P<0.05). #Significantly decreased versus CONO (P<0.05). CON= Control; CONO= Control with oxypurinol; 12MV= 12 hrs mechanical ventilation; 12MVO= 12MV with oxypurinol; 18MV= 18 hrs mechanical ventilation; 18MVO= 18MV with oxypurinol.

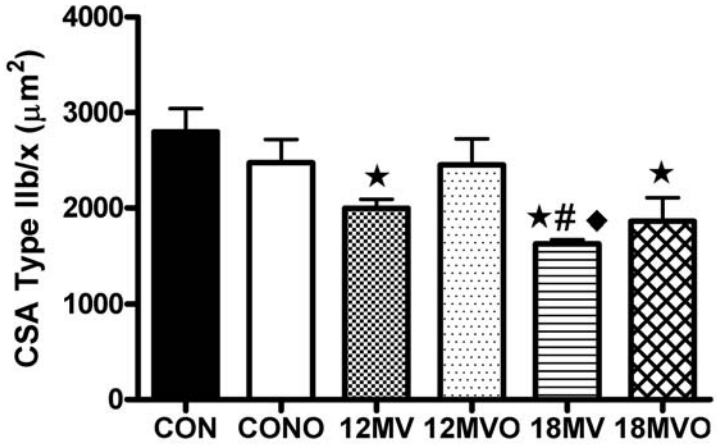

Figure 4-14. Type IIb/x fiber cross-sectional area in diaphragm samples from experiment 1. Values are mean ± SE. *Significantly decreased versus CON (P<0.05). #Significantly decreased versus CONO (P<0.05). ♦Significantly decreased versus 12MVO (P<0.05). CON= Control; CONO= Control with oxypurinol; 12MV= 12 hrs mechanical ventilation; 12MVO= 12MV with oxypurinol; 18MV= 18 hrs mechanical ventilation; 18MVO= 18MV with oxypurinol.

Table 4-3. Maximal isometric twitch force production in diaphragm strips obtained from control, mechanically ventilated, and mechanically ventilated animals with Trolox.

Experimental Group	Maximal Isometric Twitch Force, N/cm^2
Control	9.55 ± 0.28
12 h of MV	6.73 ± 0.35*#
12 h of MV with Trolox	9.31 ± 0.85

Values are expressed as mean ± SE. *Significantly decreased versus Control ($P<0.05$). #Significantly decreased versus 12 h of MV with Trolox ($P<0.05$).

Table 4-4. Hypoxanthine, xanthine, and uric acid levels in control, mechanically ventilated, and mechanically ventilated animals with Trolox.

Measurement (uM/mg protein)	CON	12MV	12MVT
Hypoxanthine	10.67 ± 0.36	9.01 ± 0.20*	9.29 ± 0.21*
Xanthine	24.43 ± 1.02	19.85 ± 1.09*	19.45 ± 0.47*
Uric Acid	24.67 ± 1.15	28.90 ± 1.43*	29.81 ± 0.72*

Values are expressed as mean ± SE. *Significantly different versus CON ($P<0.05$). CON= Control; 12MV= 12 hrs of mechanical ventilation; 12MVT= 12MV with Trolox.

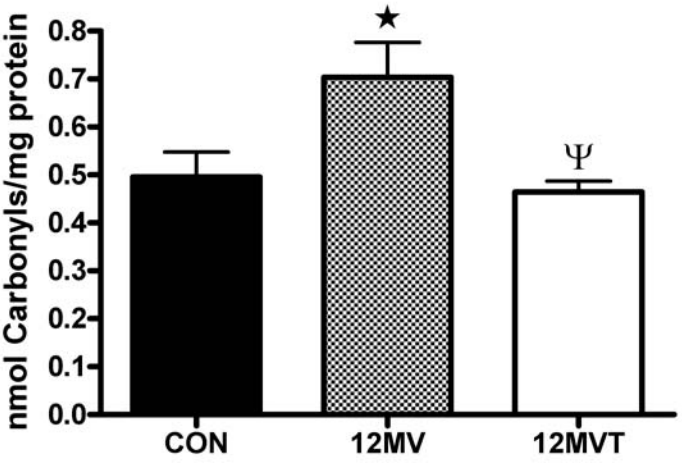

Figure 4-15. Protein carbonyl levels in diaphragm samples from experiment 2. Values are mean ± SE. *Significantly increased versus CON (P<0.05). Ψ Significantly decreased versus 12MV (P<0.05). CON= Control; 12MV= 12 hrs mechanical ventilation; 12MVT= 12MV with Trolox.

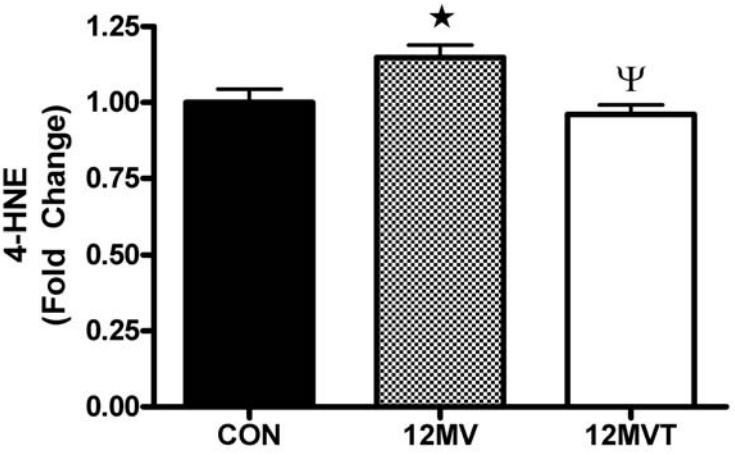

Figure 4-16. Fold changes (versus control) of 4- hydroxynonenal (4-HNE) accumulation in diaphragm samples from experiment 2. Values are mean fold change ± SE. *Significantly increased versus CON (P<0.05). Ψ Significantly decreased versus 12MV (P<0.05). CON= Control; 12MV= 12 hrs mechanical ventilation; 12MVT= 12MV with Trolox.

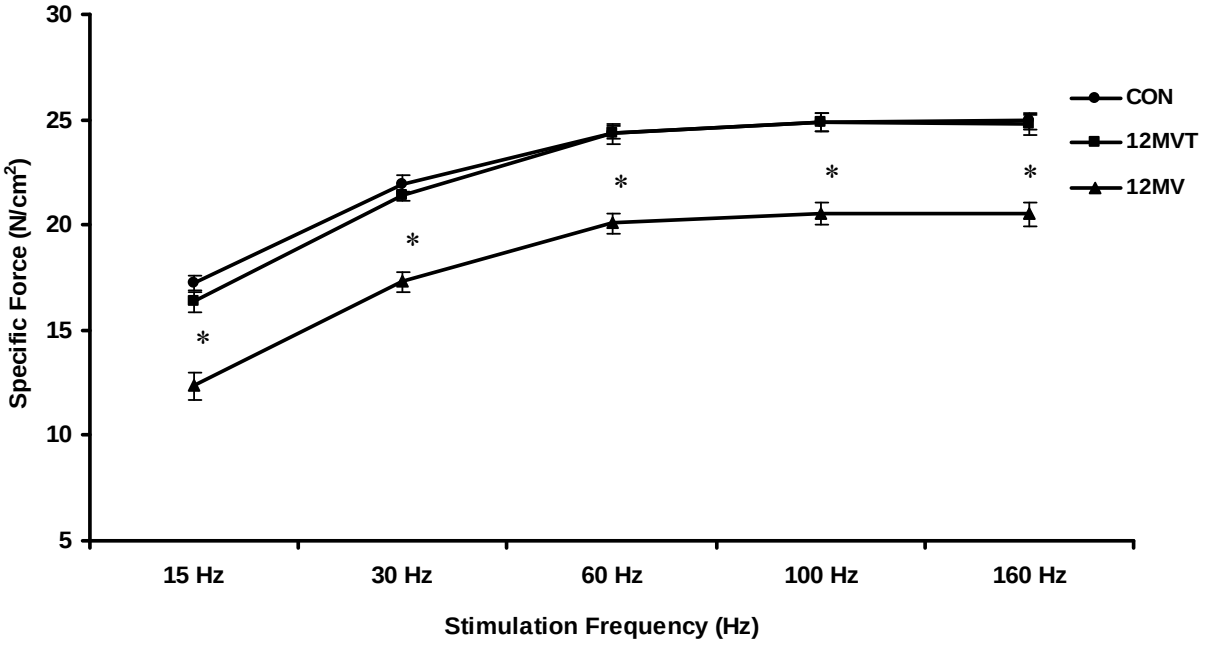

Figure 4-17. Diaphragmatic force-frequency response (*in vitro*) of diaphragm samples from experiment 2. Values are expressed as mean ± SE. *Significantly decreased versus CON and 12MVT (P<0.001). CON= Control; 12MV= 12 hrs mechanical ventilation; 12MVT= 12MV with Trolox.

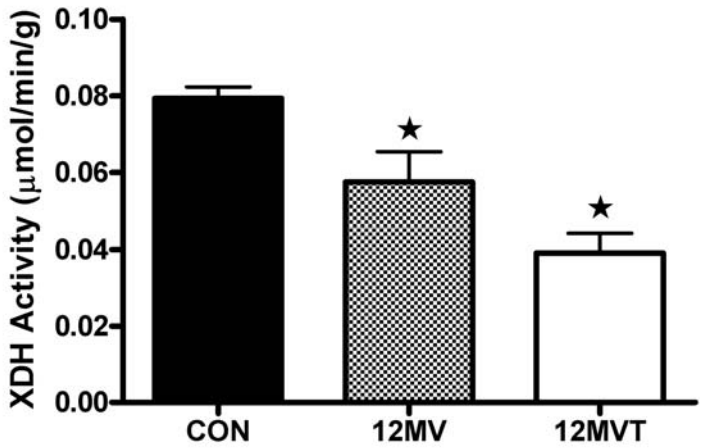

Figure 4-18. Xanthine dehydrogenase (XDH) activity in diaphragm samples from experiment 2. Values are mean fold change ± SE. *Significantly decreased versus CON (P<0.05). CON= Control; 12MV= 12 hrs mechanical ventilation; 12MVT= 12MV with Trolox.

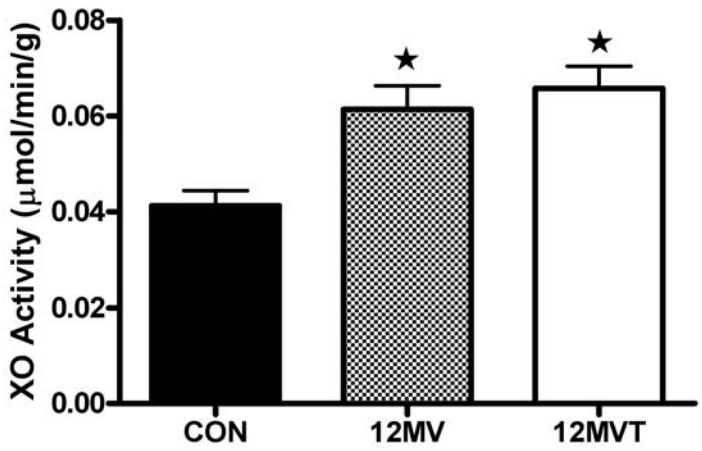

Figure 4-19. Xanthine oxidase (XO) activity in diaphragm samples from experiment 2. Values are mean fold change ± SE. *Significantly increased versus CON ($P<0.05$). CON= Control; 12MV= 12 hrs mechanical ventilation; 12MVT= 12MV with Trolox.

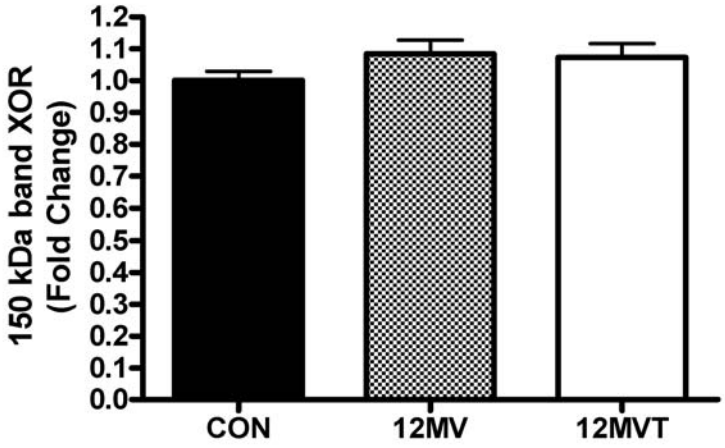

Figure 4-20. Fold changes (versus control) of XOR protein (150 kDa band) content in diaphragm samples from experiment 2. Values are mean fold change ± SE. CON= Control; 12MV= 12 hrs mechanical ventilation; 12MVT= 12MV with Trolox.

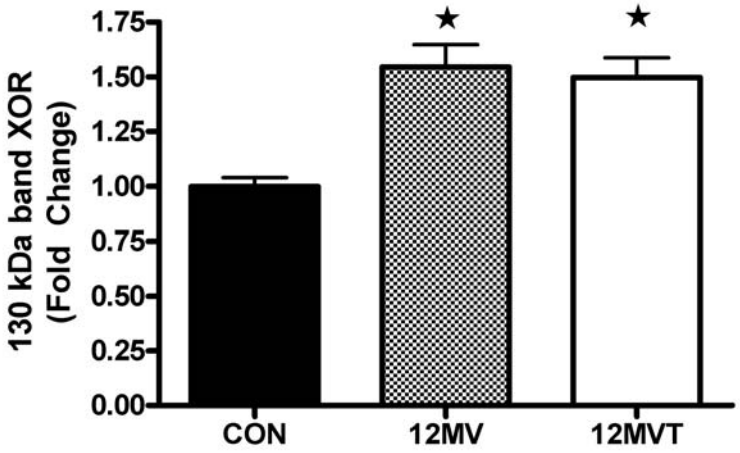

Figure 4-21. Fold changes (versus control) of XOR protein (130 kDa band) content in diaphragm samples from experiment 2. Values are mean fold change ± SE. *Significantly increased versus CON ($P<0.01$). CON= Control; 12MV= 12 hrs mechanical ventilation; 12MVT= 12MV with Trolox.

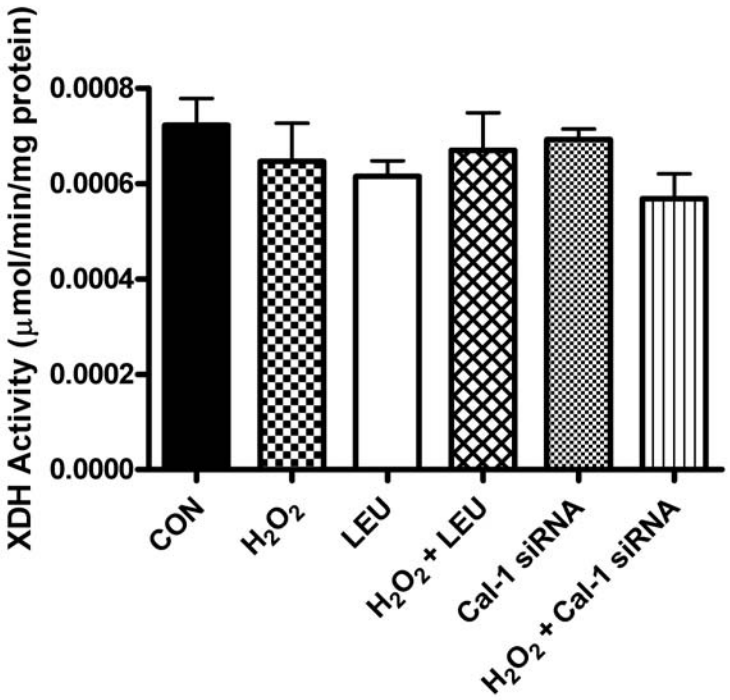

Figure 4-22. Xanthine dehydrogenase (XDH) activity in C_2C_{12} myotubes from experiment 3. Values are mean fold change ± SE. CON= Control; H_2O_2= Hydrogen peroxide; LEU= Leupeptin; H_2O_2 + LEU= Hydrogen peroxide and leupeptin; Cal-1 siRNA= Calpain-1 siRNA; H_2O_2 + Cal-1 siRNA= Hydrogen peroxide and Calpain-1 siRNA.

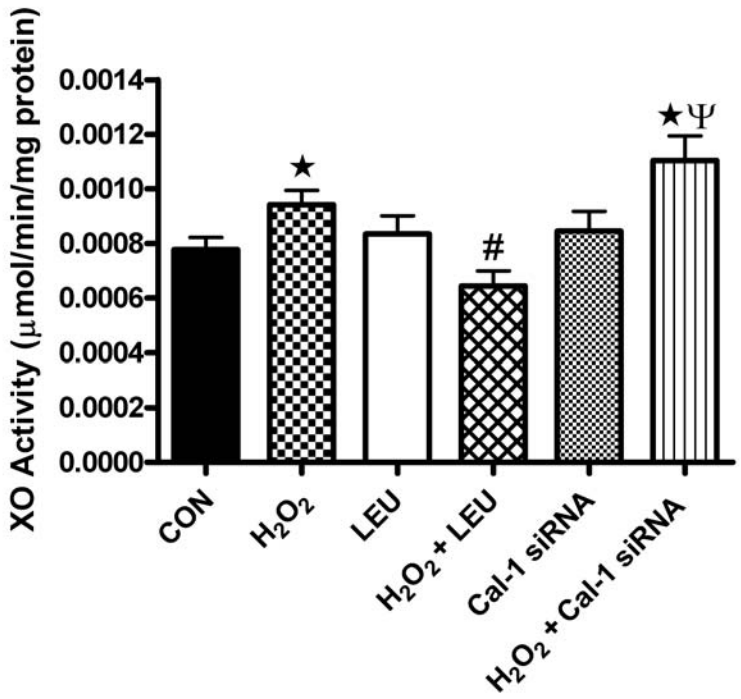

Figure 4-23. Xanthine oxidase (XO) activity in C_2C_{12} myotubes from experiment 3. Values are mean fold change ± SE. *Significantly increased versus CON ($P<0.05$). $^{\#}$Significantly decreased versus H_2O_2 ($P<0.05$). $^{\Psi}$Significantly increased versus H_2O_2 + LEU ($P<0.001$). CON= Control; H_2O_2= Hydrogen peroxide; LEU= Leupeptin; H_2O_2 + LEU= Hydrogen peroxide and leupeptin; Cal-1 siRNA= Calpain-1 siRNA; H_2O_2 + Cal-1 siRNA= Hydrogen peroxide and Calpain-1 siRNA.

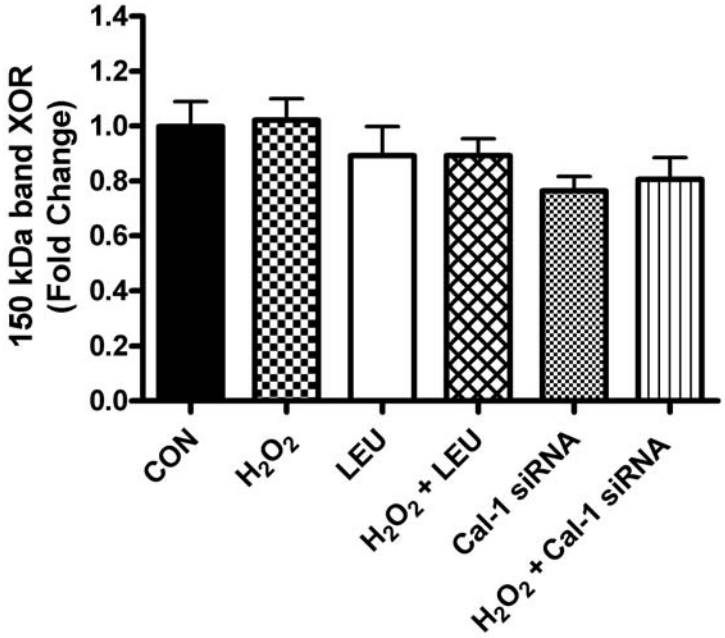

Figure 4-24. Fold change (versus control) of XOR protein (150 kDa band) in C_2C_{12} myotubes from experiment 3. Values are mean fold change ± SE. CON= Control; H_2O_2= Hydrogen peroxide; LEU= Leupeptin; H_2O_2 + LEU= Hydrogen peroxide and leupeptin; Cal-1 siRNA= Calpain-1 siRNA; H_2O_2 + Cal-1 siRNA= Hydrogen peroxide and Calpain-1 siRNA.

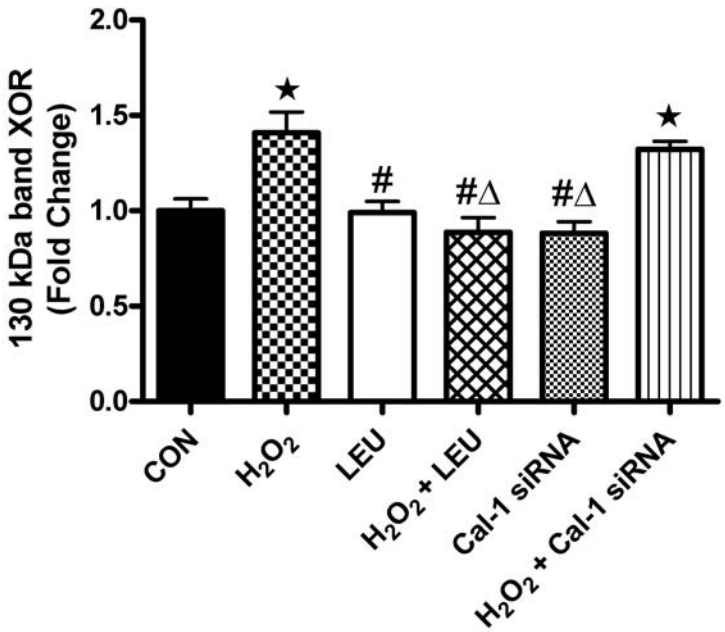

Figure 4-25. Fold change (versus control) of XOR protein (130 kDa band) in C_2C_{12} myotubes from experiment 3. Values are mean fold change ± SE. *Significantly increased versus CON ($P<0.05$). $^{\#}$Significantly decreased versus H_2O_2 ($P< 0.05$). $^{\Delta}$Significantly decreased versus H_2O_2 + Cal-1 siRNA ($P<0.05$). CON= Control; H_2O_2= Hydrogen peroxide; LEU= Leupeptin; H_2O_2 + LEU= Hydrogen peroxide and leupeptin; Cal-1 siRNA= Calpain-1 siRNA; H_2O_2 + Cal-1 siRNA= Hydrogen peroxide and Calpain-1 siRNA.

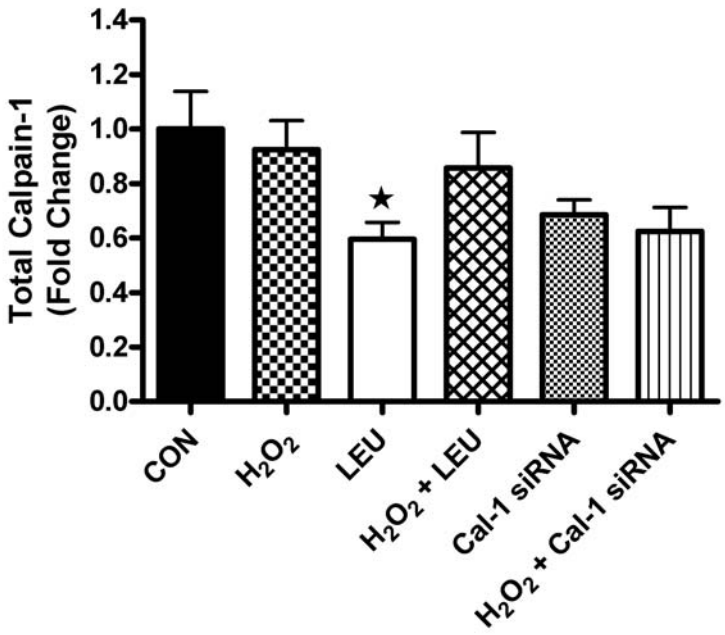

Figure 4-26. Fold change (versus control) of total calpain-1 protein in C_2C_{12} myotubes from experiment 3. Values are mean fold change ± SE. *Significantly decreased versus CON ($P<0.05$). CON= Control; H_2O_2= Hydrogen peroxide; LEU= Leupeptin; H_2O_2 + LEU= Hydrogen peroxide and leupeptin; Cal-1 siRNA= Calpain-1 siRNA; H_2O_2 + Cal-1 siRNA= Hydrogen peroxide and Calpain-1 siRNA.

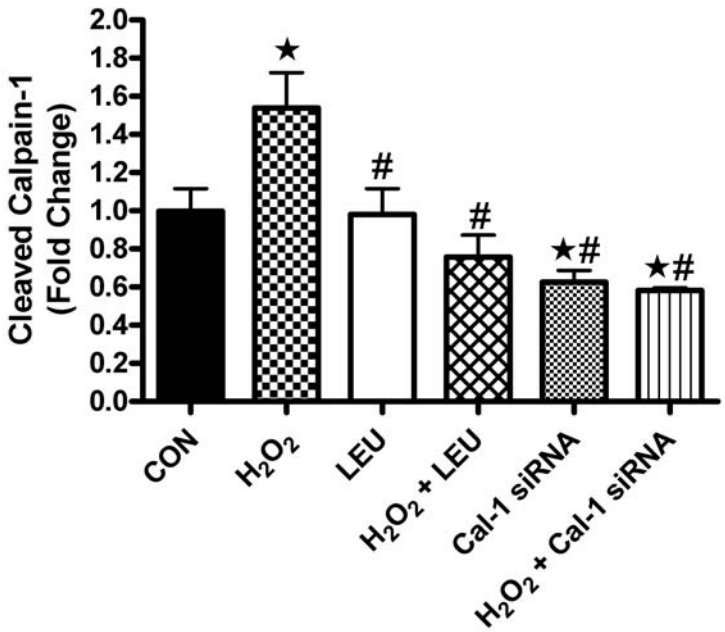

Figure 4-27. Fold change (versus control) of cleaved calpain-1 protein in C_2C_{12} myotubes from experiment 3. Values are mean fold change ± SE. *Significantly different versus CON ($P<0.05$). #Significantly decreased versus H_2O_2 ($P<0.05$). CON= Control; H_2O_2= Hydrogen peroxide; LEU= Leupeptin; H_2O_2 + LEU= Hydrogen peroxide and leupeptin; Cal-1 siRNA= Calpain-1 siRNA; H_2O_2 + Cal-1 siRNA= Hydrogen peroxide and Calpain-1 siRNA.

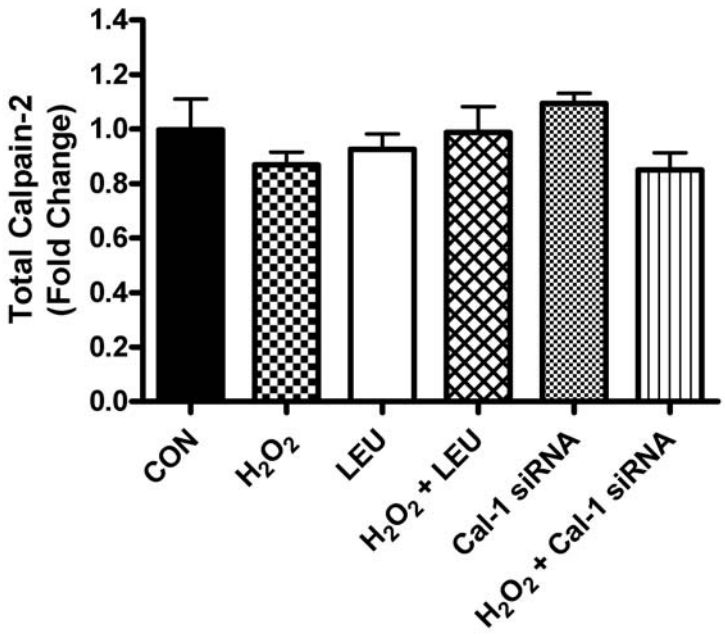

Figure 4-28. Fold change (versus control) of total calpain-2 protein in C_2C_{12} myotubes from experiment 3. Values are mean fold change ± SE. CON= Control; H_2O_2= Hydrogen peroxide; LEU= Leupeptin; H_2O_2 + LEU= Hydrogen peroxide and leupeptin; Cal-1 siRNA= Calpain-1 siRNA; H_2O_2 + Cal-1 siRNA= Hydrogen peroxide and Calpain-1 siRNA.

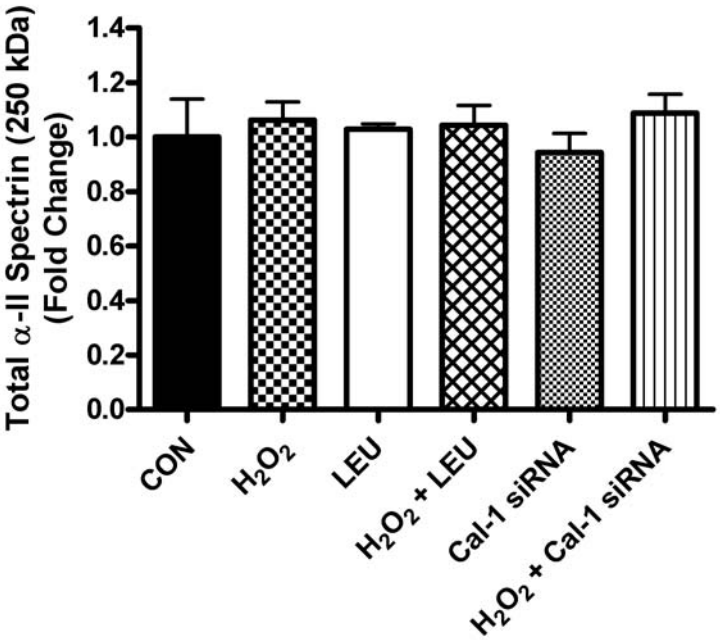

Figure 4-29. Fold change (versus control) of total α-II spectrin protein (250 kDa) in C_2C_{12} myotubes from experiment 3. Values are mean fold change ± SE. CON= Control; H_2O_2= Hydrogen peroxide; LEU= Leupeptin; H_2O_2 + LEU= Hydrogen peroxide and leupeptin; Cal-1 siRNA= Calpain-1 siRNA; H_2O_2 + Cal-1 siRNA= Hydrogen peroxide and Calpain-1 siRNA.

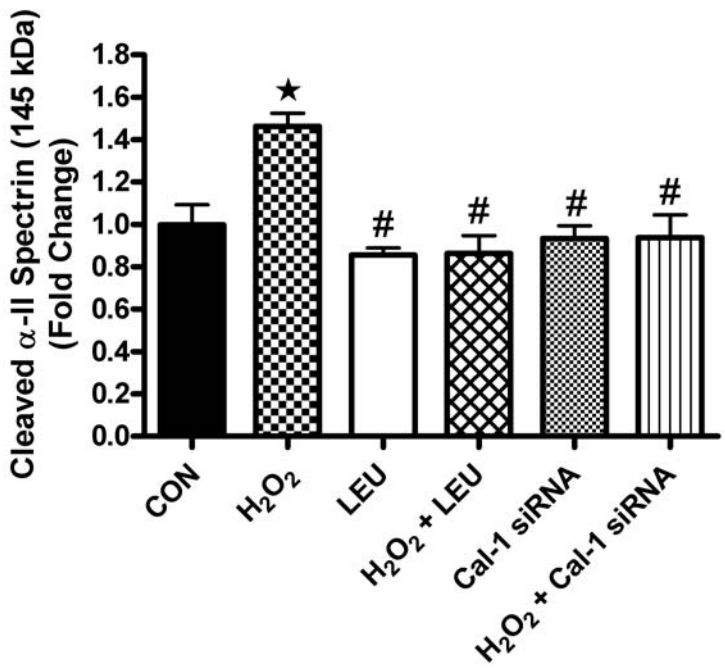

Figure 4-30. Fold change (versus control) of calpain-specific cleaved α-II spectrin protein (145 kDa) in C_2C_{12} myotubes from experiment 3. Values are mean fold change ± SE. *Significantly increased versus CON ($P<0.01$). #Significantly decreased versus H_2O_2 ($P<0.01$). CON= Control; H_2O_2= Hydrogen peroxide; LEU= Leupeptin; H_2O_2 + LEU= Hydrogen peroxide and leupeptin; Cal-1 siRNA= Calpain-1 siRNA; H_2O_2 + Cal-1 siRNA= Hydrogen peroxide and Calpain-1 siRNA.

CHAPTER 5
DISCUSSION

Overview of Principal Findings

These experiments provide new and important information regarding the impact of the XO pathway on oxidant production in the diaphragm during prolonged MV. We tested the hypothesis that XO inhibition would attenuate MV-induced diaphragmatic oxidative stress and contractile dysfunction. Our findings support this postulate as MV resulted in the up-regulation of diaphragmatic XO activity and XO inhibition attenuated some of the MV-induced oxidative stress and contractile dysfunction that is normally observed in the diaphragm. We also predicted that the administration of an exogenous antioxidant during MV would maintain redox balance in the diaphragm and retard XO activation via the reversible conversion of XDH to XO. However, our results did not support this postulate as Trolox administration failed to attenuate the MV-induced increase in XO activity and uric acid formation in the diaphragm. Finally, to investigate the activation mechanism(s) of XO in skeletal muscle, we utilized a myogenic cell line to examine the effect of a ROS challenge on XO activation in skeletal muscle myotubes. Our results indicate that hydrogen peroxide treatment of C_2C_{12}s results in the irreversible proteolytic conversion of XDH to XO. Furthermore, calpain-1 specifically does not play a role in the irreversible proteolytic conversion of XDH to XO in skeletal muscle myotubes. A detailed discussion providing an interpretation of our experiments follows in the subsequent sections.

Mechanical Ventilation-induced Induction of XO Activity

The xanthine oxidoreductase (XOR) family, which consists of xanthine dehydrogenase (XDH) and xanthine oxidase (XO), is present in almost all mammalian tissues. The enzyme catalyzes the breakdown of hypoxanthine and xanthine to urate. Importantly, the oxidase form of XOR, xanthine oxidase, produces superoxide in the catabolism of the purine substrates to uric

acid. Therefore, the XO pathway is one of the major sources of free radicals in biological systems. To examine the XO pathway during MV, we measured both XDH and XO activities in the diaphragm. Our findings show that diaphragmatic XO activity is increased during MV as shown by the increase in XO enzymatic activity and XO protein expression (130 kDa band) in the diaphragm. Moreover, hypoxanthine and xanthine, substrates for XO, were depleted in the diaphragms of our ventilated animals while uric acid, an end product of enzymatic activity, was significantly elevated.

Interestingly, prolonged (18 hrs) MV resulted in a pronounced increase in the 150 kDa band of XOR along with a concomitant increase in total XOR activity in the diaphragm. This may have been the result of an increase in XOR protein synthesis and/or a decrease in XOR protein degradation during prolonged MV. However, these experiments do not reveal the exact mechanism for increased XOR protein expression during prolonged MV.

Pharmacological inhibition of XO via oxypurinol administration attenuated the MV-induced induction of diaphragmatic XO activity and uric acid formation. As expected, oxypurinol administration had no effect on the protein levels of XO (130 kDa band of XOR) in the diaphragm but interestingly increased the induction of the 150 kDa band of XOR following ventilation. Consequently, XO inhibition during MV may produce a feedback system in which the diaphragm muscle produces more XOR protein to overcompensate for the pharmacological-induced inhibition of enzymatic activity. Overall, the MV-induced induction of diaphragmatic XO activity was abolished with oxypurinol administration.

XO Inhibition during MV Attenuates Diaphragmatic Oxidative Stress and Contractile Dysfunction

Previous work from our laboratory has revealed that MV promotes diaphragmatic oxidative injury and contractile dysfunction (12, 20, 31, 80, 81, 98, 108, 110, 122, 132). Therefore, we postulated that if diaphragmatic XO activity was induced during MV, XO-mediated oxidant production would contribute to the MV-induced diaphragmatic oxidative stress and contractile dysfunction that is normally observed. First, we confirmed our earlier reports by showing that our MV animals exhibited an increased level of oxidant production in the diaphragm when compared with control as both protein oxidation and lipid peroxidation increased with MV. However, for the first time we have shown that XO inhibition significantly reduces protein oxidation and lipid peroxidation in the diaphragm during MV. While oxypurinol administration did not completely attenuate MV-induced protein oxidation in the diaphragm, oxypurinol significantly blunted the appearance of 4-hydroxynonenal modified proteins.

The failure of oxypurinol to completely prevent oxidative stress in the diaphragm during MV does not appear to be due to an ineffective dose of oxypurinol. Indeed, it has been reported that, oral oxypurinol treatment of 50 mg/kg/day for 2 days, provides an extracellular fluid concentration of 10 μM oxypurinol and that this concentration is sufficient to cause a >80% inhibition of XO activity without a scavenging effect (134). Thus our findings indicate that our dose of oxypurinol effectively inhibited purine substrate binding and prevented the enzyme from catalyzing the conversion of the substrates into superoxide and uric acid. The observation that oxypurinol only inhibited some of the oxidative stress in the diaphragm during MV supports our hypothesis that XO plays a role in the production of ROS in the diaphragm during MV but suggests that XO is not the only source of ROS in the diaphragm.

Based upon our finding that XO inhibition was associated with decreased oxidative stress in the diaphragm, we anticipated that XO inhibition would significantly attenuate the contractile dysfunction that is normally observed with MV. Our results support this notion as XO inhibition attenuated the decrease in diaphragmatic specific force at stimulation frequencies above 60 hertz. This result is in agreement with Matuszczak and colleagues who found that XO inhibition via allopurinol lessened contractile dysfunction of skeletal muscle caused by prolonged unloading (78).

The fact that oxypurinol administration during MV attenuated both diaphragmatic XO activity levels and improved contractile function suggests that free radical damage contributed to the contractile dysfunction. In particular, oxidative modification of myosin and/or actin is a potential cause of mechanical dysfunction given their critical role in the contractile machinery. The observation that oxypurinol therapy improved isometric twitch force and shifted the force-frequency curve toward control suggests a direct effect of oxypurinol in attenuating contractile protein oxidation. A similar finding was noted recently by Kogler et al. who found that oxypurinol enhanced cardiac muscle twitch tension in spontaneously hypertensive, heart failure-prone rats without alterations in intracellular calcium amplitudes (59).

While XO inhibition prevented some of the decrease in diaphragmatic dysfunction, it did not completely restore contractile function to control. The partial protection of contractile function with XO inhibition may be due to ROS generation from additional pathways. In our MV model, XO may work in conjunction with other oxidant producing pathways (i.e., heme-oxygenase-1 and mitochondria) in the diaphragm to generate free radicals. This theory is logical given that oxypurinol only inhibits XO activity and does not inhibit ROS production from other oxidant producing pathways and the fact that the MV-induced oxidative stress was not

completely restored with XO inhibition. Accordingly, ROS generation from another pathway could theoretically contribute to both the MV-induced oxidative stress and contractile dysfunction that is observed in the diaphragm that is not restored with XO inhibition.

Antioxidant Administration during MV Fails to Attenuate XO Activation

Mammalian XORs (XDH & XO) catalyze the hydroxylation of hypoxanthine and xanthine at the molybdenum center of the enzyme and reducing equivalents thus introduced into the enzymes are transferred via two iron sulfur centers to flavin adenine dinucleotide (FAD), where the reduction of NAD+ or molecular oxygen occurs (60). These enzymes are synthesized as the dehydrogenase form (XDH) but can be readily converted to the oxidase form (XO) reversibly by oxidation of sulfhydryl residues or irreversibly by proteolysis (2, 22, 91, 114). During the reversible XDH to XO conversion, oxidation of cysteines residues on XDH results in the displacement of an active loop around FAD. The displacement of this loop blocks the approach of the pyridine ring of the NAD+ substrate to the isoalloxazine ring of the enzymes cofactor and changes the electrostatic environment around FAD. Thus the movement of the active loop causes the reversible conversion of XDH to XO (27). Therefore, the reversible conversion of XDH to XO via the oxidation of cysteine residues on XOR changes enzymatic function but does not change the enzymes molecular weight. Hence, it is feasible that during MV XO activity may be up-regulated via the oxidation of XDH to XO. Once again, pathways other than XO may generate ROS during MV and the oxidants from one of those pathways may be responsible for the reversible activation of XO.

In an attempt to understand the reversible conversion mechanism by which XO activity maybe increased in the diaphragm during MV, we used the pharmacological agent Trolox to maintain redox balance. Trolox is a water soluble Vitamin E analog that has been shown to

reduce MV-induced oxidative stress and contractile dysfunction (12, 80, 81). So initially, we confirmed our earlier reports by showing that Trolox administration effectively attenuated both protein oxidation and lipid peroxidation in the diaphragm during MV. Second, we demonstrated the ability of Trolox to attenuate all of the contractile dysfunction that is normally observed with 12 hours of MV. As a result, our use of Trolox as a means to restore redox balance in the diaphragm was achieved in this experiment.

Because Trolox administration attenuated the MV-induced oxidative stress in the diaphragm, we hypothesized that the MV-induced induction of XO activity would be blunted by the elimination of the reversible conversion of XDH to XO via oxidation. However, Trolox administration during MV failed to attenuate either the increase in XO activity in the diaphragm during MV or the increase in uric acid formation. Furthermore neither the levels of hypoxanthine or xanthine were changed in the animals treated with Trolox. Hence, the restoration of redox balance with Trolox does not affect the increase in diaphragmatic XO activity during MV.

It is important to note that our MV duration may not have been adequate to examine the reversible conversion of XDH to XO in the diaphragm. Specifically, the irreversible proteolytic processing of XDH results in the cleavage of a 15-20 kDa fragment from the enzyme resulting in the appearance of the active 130 kDa band of XOR (22, 130). During this conversion, the active loop around FAD is moved resulting in an electrostatic environment that favors the use of only molecular oxygen in the reduction of the purine substrates. Importantly, this proteolytic process is believed to occur subsequent to the reversible conversion (14, 83). Because the irreversible proteolytic conversion of XDH to XO is present in the diaphragm during MV, as demonstrated by the increase in diaphragmatic XO activity along with the induction of the 130 kDa band of

XOR, we may have missed the reversible conversion of XDH to XO in our model because our ventilation was too long. Perhaps the reversible conversion of XDH to XO in the diaphragm would be adequately observed following 3 or 6 hours of MV.

Hydrogen Peroxide Activates XO in Myotubes

Oxidant challenges (H_2O_2) to C_2C_{12} myotubes can induce oxidative stress and proteolysis (74, 116). In addition, hydrogen peroxide has been shown to modulate the reversible conversion of XDH to XO in non-muscle cell lines (85). Therefore, as a means of providing a controlled *in vitro* environment to study the activation mechanism(s) of XO with a H_2O_2 challenge, we included a myogenic cell culture model in our experiments. Specifically, we tested the hypothesis that exposure of skeletal muscle myotubes to hydrogen peroxide (100 μM) would increase XO activity via the oxidative modification of XDH to XO. Our results indicate that hydrogen peroxide increases the proteolytic conversion of XDH to XO via the induction of the active form of XO protein (130 kDa band) in conjunction with increases in XO activity. These results are similar to our *in vivo* results whereby XO activity was increased in the diaphragms of our MV animals. While indicating that the irreversible process is increased in our *in vitro* model, these results fail to specifically identify the protease responsible for the induction of the 130 kDa band of XOR.

Knowing that hydrogen peroxide increases calpain activity in our C_2C_{12} cell line, we inhibited calpain activity in our cell culture experiments using both leupeptin and short interference RNA (siRNA) to focus solely on the oxidative challenge presented by hydrogen peroxide treatment. Leupeptin is an inhibitor of lysosomal thiol proteases and calcium-activated proteases (77). Specifically, leupeptin inhibits papain, cathepsin B, endoproteinase Lys-C, and calpain. Interestingly, we found that when cells were treated with both hydrogen peroxide and

leupeptin, the hydrogen peroxide-induced increases in both XO activity and protein expression were significantly attenuated, suggesting that the irreversible proteolytic conversion of XDH to XO in skeletal muscle myotubes with a ROS challenge (H_2O_2) involves either a lysosomal or calpain protease.

Short interference RNA (siRNA) for calpain-1 was also used to inhibit the hydrogen peroxide-induced increase in calpain activity in our C_2C_{12} cell line. siRNA is used to interfere with the expression of the calpain-1 gene. We found that cells treated with both hydrogen peroxide and siRNA for calpain-1 exhibited the same increase in the 130 kDa band of XOR in concomitant with an increase in XO activity as cells treated with only hydrogen peroxide, proving that the irreversible conversion of XDH to XO via a ROS challenge does not involve calpain-1 activation.

Our cell culture results coincide with work by McNally et al. who found that H_2O_2 markedly enhances the irreversible conversion of XDH to XO in endothelial cells (85). In addition, with respect to MV, our cell culture experiments shed light on the observation that leupeptin can inhibit ventilator-induced diaphragm dysfunction in rats (77). Perhaps leupeptin prevents the induction of XO activity in the *in vivo* MV model and prevents XO-mediated ROS production. However, our results do not agree with a study performed on human liver by Saksela et al (102). While these researchers suggest that excess intracellular calcium is involved in the XDH to XO conversion in human liver, they predict that a mitochondrial protease is responsible for the proteolytic cleavage of XDH to XO. In an ischemia-reperfusion model, they theorized that an intracellular calcium influx produced by reperfusion would damage the mitochondria resulting in the opening of the mitochondrial permeability transition pore and result in the release of mitochondrial proteins into the cytoplasm (102). While these researchers failed

to identify the specific mitochondrial protease, a study by Sitte et al. recently characterized a mitochondrial intermembrane protease isolated from rat liver that is significantly inhibited by leupeptin (111). Additional work is required to determine if a mitochondrial protease is responsible for activation of XO in myotubes exposed to a ROS challenge.

Conclusions and Future Directions

This study provides the first *in vivo* evidence that diaphragmatic XO activity contributes to MV-induced oxidative stress and contractile dysfunction. Specifically, these results demonstrate that XO inhibition attenuates MV-induced oxidative stress and eliminates some of the contractile dysfunction that is normally observed with MV. Furthermore, XO is up-regulated in the diaphragm by the irreversible proteolytic cleavage of XDH to XO during MV. Finally, the irreversible conversion of XDH to XO in skeletal muscle myotubes induced by a ROS challenge (H_2O_2) is a calpain-1-independent process. Collectively, these are novel and important findings. In fact, prior to the current experiments, the question of whether XO contributes to MV-induced oxidative damage in the diaphragm remained unknown. Our results clearly indicate that XO-mediated production of superoxide is involved in MV-induced diaphragmatic oxidative stress and contractile dysfunction. Moreover, our findings suggest that pharmacological inhibition of XO activity could be a potential therapeutic strategy to retard MV-induced oxidative stress and contractile dysfunction in the diaphragm during prolonged MV. This is clinically significant because MV-induced diaphragmatic weakness plays an important role in weaning difficulties following MV.

Future studies should focus on elucidating the protease that is responsible for the proteolytic cleavage of XDH to XO in skeletal muscle and effectively determine if the reversible conversion of XDH to XO via oxidation is an essential first step in the activation of XO activity in skeletal muscle under conditions of disuse. A complete understanding of these two important

issues is essential to fully understand the XO pathway in skeletal muscle. Specifically, the complete understanding of the XO pathway in the diaphragm during MV will be beneficial in the development of effective and safe countermeasures for preventing respiratory muscle weakness during prolonged MV. The development of a therapeutic strategy to retard MV-induced diaphragmatic oxidative damage and weakness would likely result in the maintenance of adequate inspiratory muscle function and result in higher weaning success rates.

LIST OF REFERENCES

1. **Ajamieh H, Merino N, Candelario-Jalil E, Menendez S, Martinez-Sanchez G, Re L, Giuliani A, and Leon OS.** Similar protective effect of ischaemic and ozone oxidative preconditionings in liver ischaemia/reperfusion injury. *Pharmacol Res* 45: 333-339, 2002.

2. **Amaya Y, Yamazaki K, Sato M, Noda K, and Nishino T.** Proteolytic conversion of xanthine dehydrogenase from the NAD-dependent type to the O2-dependent type. Amino acid sequence of rat liver xanthine dehydrogenase and identification of the cleavage sites of the enzyme protein during irreversible conversion by trypsin. *J Biol Chem* 265: 14170-14175, 1990.

3. **Andreyev AY, Kushnareva YE, and Starkov AA.** Mitochondrial metabolism of reactive oxygen species. *Biochemistry (Mosc)* 70: 200-214, 2005.

4. **Anzueto A, Peters JI, Tobin MJ, de los Santos R, Seidenfeld JJ, Moore G, Cox WJ, and Coalson JJ.** Effects of prolonged controlled mechanical ventilation on diaphragmatic function in healthy adult baboons. *Crit Care Med* 25: 1187-1190, 1997.

5. **Attaix D, Ventadour S, Codran A, Bechet D, Taillandier D, and Combaret L.** The ubiquitin-proteasome system and skeletal muscle wasting. *Essays Biochem* 41: 173-186, 2005.

6. **Baar K, Nader G, and Bodine S.** Resistance exercise, muscle loading/unloading and the control of muscle mass. *Essays Biochem* 42: 61-74, 2006.

7. **Barreiro E, Comtois AS, Gea J, Laubach VE, and Hussain SN.** Protein tyrosine nitration in the ventilatory muscles: role of nitric oxide synthases. *Am J Respir Cell Mol Biol* 26: 438-446, 2002.

8. **Bartoli M and Richard I.** Calpains in muscle wasting. *Int J Biochem Cell Biol* 37: 2115-2133, 2005.

9. **Beckman JS, Parks DA, Pearson JD, Marshall PA, and Freeman BA.** A sensitive fluorometric assay for measuring xanthine dehydrogenase and oxidase in tissues. *Free Radic Biol Med* 6: 607-615, 1989.

10. **Bernard N, Matecki S, Py G, Lopez S, Mercier J, and Capdevila X.** Effects of prolonged mechanical ventilation on respiratory muscle ultrastructure and mitochondrial respiration in rabbits. *Intensive Care Med* 29: 111-118, 2003.

11. **Berry CE and Hare JM.** Xanthine oxidoreductase and cardiovascular disease: molecular mechanisms and pathophysiological implications. *J Physiol* 555: 589-606, 2004.

12. **Betters JL, Criswell DS, Shanely RA, Van Gammeren D, Falk D, Deruisseau KC, Deering M, Yimlamai T, and Powers SK.** Trolox attenuates mechanical ventilation-induced diaphragmatic dysfunction and proteolysis. *Am J Respir Crit Care Med* 170: 1179-1184, 2004.

13. **Bodine SC, Latres E, Baumhueter S, Lai VK, Nunez L, Clarke BA, Poueymirou WT, Panaro FJ, Na E, Dharmarajan K, Pan ZQ, Valenzuela DM, DeChiara TM, Stitt TN, Yancopoulos GD, and Glass DJ.** Identification of ubiquitin ligases required for skeletal muscle atrophy. *Science* 294: 1704-1708, 2001.

14. **Brass CA, Narciso J, and Gollan JL.** Enhanced activity of the free radical producing enzyme xanthine oxidase in hypoxic rat liver. Regulation and pathophysiologic significance. *J Clin Invest* 87: 424-431, 1991.

15. **Bray R.** Molybdenum iron-sulfur flavin hydroxylases and related enzymes. In: *The enzymes*. New York: Academic Press, 1975, p. 229-419.

16. **Cadenas E and Davies KJ.** Mitochondrial free radical generation, oxidative stress, and aging. *Free Radic Biol Med* 29: 222-230, 2000.

17. **Chevrolet JC.** Difficult weaning from mechanical ventilation. *Lung* 168 Suppl: 829-832, 1990.

18. **Clark JE, Foresti R, Green CJ, and Motterlini R.** Dynamics of haem oxygenase-1 expression and bilirubin production in cellular protection against oxidative stress. *Biochem J* 348 Pt 3: 615-619, 2000.

19. **Communal C, Sumandea M, de Tombe P, Narula J, Solaro RJ, and Hajjar RJ.** Functional consequences of caspase activation in cardiac myocytes. *Proc Natl Acad Sci U S A* 99: 6252-6256, 2002.

20. **Criswell DS, Shanely RA, Betters JJ, McKenzie MJ, Sellman JE, Van Gammeren DL, and Powers SK.** Cumulative effects of aging and mechanical ventilation on in vitro diaphragm function. *Chest* 124: 2302-2308, 2003.

21. **Dedieu S, Poussard S, Mazeres G, Grise F, Dargelos E, Cottin P, and Brustis JJ.** Myoblast migration is regulated by calpain through its involvement in cell attachment and cytoskeletal organization. *Exp Cell Res* 292: 187-200, 2004.

22. **Della Corte E and Stirpe F.** The regulation of rat-liver xanthine oxidase: Activation by proteolytic enzymes. *FEBS Lett* 2: 83-84, 1968.

23. **DeRuisseau KC, Kavazis AN, Deering MA, Falk DJ, Van Gammeren D, Yimlamai T, Ordway GA, and Powers SK.** Mechanical ventilation induces alterations of the ubiquitin-proteasome pathway in the diaphragm. *J Appl Physiol* 98: 1314-1321, 2005.

24. **Dodd SL, Powers SK, Vrabas IS, Criswell D, Stetson S, and Hussain R.** Effects of clenbuterol on contractile and biochemical properties of skeletal muscle. *Med Sci Sports Exerc* 28: 669-676, 1996.

25. **Dorion D, Zhong A, Chiu C, Forrest CR, Boyd B, and Pang CY.** Role of xanthine oxidase in reperfusion injury of ischemic skeletal muscles in the pig and human. *J Appl Physiol* 75: 246-255, 1993.

26. **Duan X, Berthiaume F, Yarmush D, and Yarmush ML.** Proteomic analysis of altered protein expression in skeletal muscle of rats in a hypermetabolic state induced by burn sepsis. *Biochem J* 397: 149-158, 2006.

27. **Enroth C, Eger BT, Okamoto K, Nishino T, and Pai EF.** Crystal structures of bovine milk xanthine dehydrogenase and xanthine oxidase: structure-based mechanism of conversion. *Proc Natl Acad Sci U S A* 97: 10723-10728, 2000.

28. **Erdei N, Toth A, Pasztor ET, Papp Z, Edes I, Koller A, and Bagi Z.** High-fat diet-induced reduction in nitric oxide-dependent arteriolar dilation in rats: role of xanthine oxidase-derived superoxide anion. *Am J Physiol Heart Circ Physiol* 291: H2107-2115, 2006.

29. **Esteban A, Alia I, Ibanez J, Benito S, and Tobin MJ.** Modes of mechanical ventilation and weaning. A national survey of Spanish hospitals. The Spanish Lung Failure Collaborative Group. *Chest* 106: 1188-1193, 1994.

30. **Esteban A, Anzueto A, Alia I, Gordo F, Apezteguia C, Palizas F, Cide D, Goldwaser R, Soto L, Bugedo G, Rodrigo C, Pimentel J, Raimondi G, and Tobin MJ.** How is mechanical ventilation employed in the intensive care unit? An international utilization review. *Am J Respir Crit Care Med* 161: 1450-1458, 2000.

31. **Falk DJ, Deruisseau KC, Van Gammeren DL, Deering MA, Kavazis AN, and Powers SK.** Mechanical ventilation promotes redox status alterations in the diaphragm. *J Appl Physiol* 101: 1017-1024, 2006.

32. **Fredriksson K, Radell P, Eriksson LI, Hultenby K, and Rooyackers O.** Effect of prolonged mechanical ventilation on diaphragm muscle mitochondria in piglets. *Acta Anaesthesiol Scand* 49: 1101-1107, 2005.

33. **Gayan-Ramirez G, de Paepe K, Cadot P, and Decramer M.** Detrimental effects of short-term mechanical ventilation on diaphragm function and IGF-I mRNA in rats. *Intensive Care Med* 29: 825-833, 2003.

34. **Gayan-Ramirez G and Decramer M.** Effects of mechanical ventilation on diaphragm function and biology. *Eur Respir J* 20: 1579-1586, 2002.

35. **Gomes-Marcondes MC and Tisdale MJ.** Induction of protein catabolism and the ubiquitin-proteasome pathway by mild oxidative stress. *Cancer Lett* 180: 69-74, 2002.

36. **Gomez-Cabrera MC, Borras C, Pallardo FV, Sastre J, Ji LL, and Vina J.** Decreasing xanthine oxidase-mediated oxidative stress prevents useful cellular adaptations to exercise in rats. *J Physiol* 567: 113-120, 2005.

37. **Granger DN, Hollwarth ME, and Parks DA.** Ischemia-reperfusion injury: role of oxygen-derived free radicals. *Acta Physiol Scand Suppl* 548: 47-63, 1986.

38. **Granger DN, Rutili G, and McCord JM.** Superoxide radicals in feline intestinal ischemia. *Gastroenterology* 81: 22-29, 1981.

39. **Halliwell B.** *Free Radicals in Biology and Medicine*. London: Oxford University Press, 1999.

40. **Harrison R.** Structure and function of xanthine oxidoreductase: where are we now? *Free Radic Biol Med* 33: 774-797, 2002.

41. **Hazan I, Dana R, Granot Y, and Levy R.** Cytosolic phospholipase A2 and its mode of activation in human neutrophils by opsonized zymosan. Correlation between 42/44 kDa mitogen-activated protein kinase, cytosolic phospholipase A2 and NADPH oxidase. *Biochem J* 326 (Pt 3): 867-876, 1997.

42. **Hellsten Y.** The role of xanthine oxidase in exercise. In: *Handbook of Oxidants and Antioxidants in Exercise*. Amsterdam: Elsevier Press, 2000, p. 153-176.

43. **Hellsten Y, Frandsen U, Orthenblad N, Sjodin B, and Richter EA.** Xanthine oxidase in human skeletal muscle following eccentric exercise: a role in inflammation. *J Physiol* 498 (Pt 1): 239-248, 1997.

44. **Hess D.** *Essentials of Mechanical Ventilation*. New York: McGraw-Hill, 1996.

45. **Heunks LM, Vina J, van Herwaarden CL, Folgering HT, Gimeno A, and Dekhuijzen PN.** Xanthine oxidase is involved in exercise-induced oxidative stress in chronic obstructive pulmonary disease. *Am J Physiol* 277: R1697-1704, 1999.

46. **Hille R.** The Mononuclear Molybdenum Enzymes. *Chem Rev* 96: 2757-2816, 1996.

47. **Hille R and Nishino T.** Flavoprotein structure and mechanism. 4. Xanthine oxidase and xanthine dehydrogenase. *FASEB J* 9: 995-1003, 1995.

48. **Hornberger TA, Hunter RB, Kandarian SC, and Esser KA.** Regulation of translation factors during hindlimb unloading and denervation of skeletal muscle in rats. *Am J Physiol Cell Physiol* 281: C179-187, 2001.

49. **Ibrahim B and Stoward PJ.** The histochemical localization of xanthine oxidase. *Histochem J* 10: 615-617, 1978.

50. **Isabelle M, Vergeade A, Moritz F, Dautreaux B, Henry JP, Lallemand F, Richard V, Mulder P, Thuillez C, and Monteil C.** NADPH oxidase inhibition prevents cocaine-induced up-regulation of xanthine oxidoreductase and cardiac dysfunction. *J Mol Cell Cardiol* 42: 326-332, 2007.

51. **Jaber S, Sebbane M, Koechlin C, Hayot M, Capdevila X, Eledjam JJ, Prefaut C, Ramonatxo M, and Matecki S.** Effects of short vs. prolonged mechanical ventilation on antioxidant systems in piglet diaphragm. *Intensive Care Med* 31: 1427-1433, 2005.

52. **Javesghani D, Magder SA, Barreiro E, Quinn MT, and Hussain SN.** Molecular characterization of a superoxide-generating NAD(P)H oxidase in the ventilatory muscles. *Am J Respir Crit Care Med* 165: 412-418, 2002.

53. **Judge AR and Dodd SL.** Xanthine oxidase and activated neutrophils cause oxidative damage to skeletal muscle after contractile claudication. *Am J Physiol Heart Circ Physiol* 286: H252-256, 2004.

54. **Kaminski HJ and Andrade FH.** Nitric oxide: biologic effects on muscle and role in muscle diseases. *Neuromuscul Disord* 11: 517-524, 2001.

55. **Keyse SM and Tyrrell RM.** Heme oxygenase is the major 32-kDa stress protein induced in human skin fibroblasts by UVA radiation, hydrogen peroxide, and sodium arsenite. *Proc Natl Acad Sci U S A* 86: 99-103, 1989.

56. **Khan SA, Lee K, Minhas KM, Gonzalez DR, Raju SV, Tejani AD, Li D, Berkowitz DE, and Hare JM.** Neuronal nitric oxide synthase negatively regulates xanthine oxidoreductase inhibition of cardiac excitation-contraction coupling. *Proc Natl Acad Sci U S A* 101: 15944-15948, 2004.

57. **Klein AS, Joh JW, Rangan U, Wang D, and Bulkley GB.** Allopurinol: discrimination of antioxidant from enzyme inhibitory activities. *Free Radic Biol Med* 21: 713-717, 1996.

58. **Knisely AS, Leal SM, and Singer DB.** Abnormalities of diaphragmatic muscle in neonates with ventilated lungs. *J Pediatr* 113: 1074-1077, 1988.

59. **Kogler H, Fraser H, McCune S, Altschuld R, and Marban E.** Disproportionate enhancement of myocardial contractility by the xanthine oxidase inhibitor oxypurinol in failing rat myocardium. *Cardiovasc Res* 59: 582-592, 2003.

60. **Komai H, Massey V, and Palmer G.** The preparation and properties of deflavo xanthine oxidase. *J Biol Chem* 244: 1692-1700, 1969.

61. **Kondo H, Miura M, and Itokawa Y.** Antioxidant enzyme systems in skeletal muscle atrophied by immobilization. *Pflugers Arch* 422: 404-406, 1993.

62. **Kondo H, Miura M, and Itokawa Y.** Oxidative stress in skeletal muscle atrophied by immobilization. *Acta Physiol Scand* 142: 527-528, 1991.

63. **Kondo H, Miura M, Kodama J, Ahmed SM, and Itokawa Y.** Role of iron in oxidative stress in skeletal muscle atrophied by immobilization. *Pflugers Arch* 421: 295-297, 1992.

64. **Kondo H, Miura M, Nakagaki I, Sasaki S, and Itokawa Y.** Trace element movement and oxidative stress in skeletal muscle atrophied by immobilization. *Am J Physiol* 262: E583-590, 1992.

65. **Kondo H, Nakagaki I, Sasaki S, Hori S, and Itokawa Y.** Mechanism of oxidative stress in skeletal muscle atrophied by immobilization. *Am J Physiol* 265: E839-844, 1993.

66. **Ku Z, Yang J, Menon V, and Thomason DB.** Decreased polysomal HSP-70 may slow polypeptide elongation during skeletal muscle atrophy. *Am J Physiol* 268: C1369-1374, 1995.

67. **Kvam E, Hejmadi V, Ryter S, Pourzand C, and Tyrrell RM.** Heme oxygenase activity causes transient hypersensitivity to oxidative ultraviolet A radiation that depends on release of iron from heme. *Free Radic Biol Med* 28: 1191-1196, 2000.

68. **Landmesser U, Spiekermann S, Dikalov S, Tatge H, Wilke R, Kohler C, Harrison DG, Hornig B, and Drexler H.** Vascular oxidative stress and endothelial dysfunction in patients with chronic heart failure: role of xanthine-oxidase and extracellular superoxide dismutase. *Circulation* 106: 3073-3078, 2002.

69. **Le Bourdelles G, Viires N, Boczkowski J, Seta N, Pavlovic D, and Aubier M.** Effects of mechanical ventilation on diaphragmatic contractile properties in rats. *Am J Respir Crit Care Med* 149: 1539-1544, 1994.

70. **Lemaire F.** Difficult weaning. *Intensive Care Med* 19 Suppl 2: S69-73, 1993.

71. **Levine S, Nguyen T, Taylor N, Friscia ME, Budak MT, Rothenberg P, Zhu J, Sachdeva R, Sonnad S, Kaiser LR, Rubinstein NA, Powers SK, and Shrager JB.** Rapid disuse atrophy of diaphragm fibers in mechanically ventilated humans. *N Engl J Med* 358: 1327-1335, 2008.

72. **Li YP, Atkins CM, Sweatt JD, and Reid MB.** Mitochondria mediate tumor necrosis factor-alpha/NF-kappaB signaling in skeletal muscle myotubes. *Antioxid Redox Signal* 1: 97-104, 1999.

73. **Li YP, Chen Y, John J, Moylan J, Jin B, Mann DL, and Reid MB.** TNF-alpha acts via p38 MAPK to stimulate expression of the ubiquitin ligase atrogin1/MAFbx in skeletal muscle. *FASEB J* 19: 362-370, 2005.

74. **Li YP, Chen Y, Li AS, and Reid MB.** Hydrogen peroxide stimulates ubiquitin-conjugating activity and expression of genes for specific E2 and E3 proteins in skeletal muscle myotubes. *Am J Physiol Cell Physiol* 285: C806-812, 2003.

75. **Li YP and Reid MB.** NF-kappaB mediates the protein loss induced by TNF-alpha in differentiated skeletal muscle myotubes. *Am J Physiol Regul Integr Comp Physiol* 279: R1165-1170, 2000.

76. **Li YP, Schwartz RJ, Waddell ID, Holloway BR, and Reid MB.** Skeletal muscle myocytes undergo protein loss and reactive oxygen-mediated NF-kappaB activation in response to tumor necrosis factor alpha. *FASEB J* 12: 871-880, 1998.

77. **Maes K, Testelmans D, Powers S, Decramer M, and Gayan-Ramirez G.** Leupeptin inhibits ventilator-induced diaphragm dysfunction in rats. *Am J Respir Crit Care Med* 175: 1134-1138, 2007.

78. **Matuszczak Y, Arbogast S, and Reid MB.** Allopurinol mitigates muscle contractile dysfunction caused by hindlimb unloading in mice. *Aviat Space Environ Med* 75: 581-588, 2004.

79. **McClung JM, Kavazis AN, DeRuisseau KC, Falk DJ, Deering MA, Lee Y, Sugiura T, and Powers SK.** Caspase-3 regulation of diaphragm myonuclear domain during mechanical ventilation-induced atrophy. *Am J Respir Crit Care Med* 175: 150-159, 2007.

80. **McClung JM, Kavazis AN, Whidden MA, DeRuisseau KC, Falk DJ, Criswell DS, and Powers SK.** Antioxidant administration attenuates mechanical ventilation-induced rat diaphragm muscle atrophy independent of protein kinase B (PKB Akt) signalling. *J Physiol* 585: 203-215, 2007.

81. **McClung JM, Whidden MA, Kavazis AN, Falk DJ, Deruisseau KC, and Powers SK.** Redox regulation of diaphragm proteolysis during mechanical ventilation. *Am J Physiol Regul Integr Comp Physiol*, 2008.

82. **McCord JM.** Oxygen-derived free radicals in postischemic tissue injury. *N Engl J Med* 312: 159-163, 1985.

83. **McKelvey TG, Hollwarth ME, Granger DN, Engerson TD, Landler U, and Jones HP.** Mechanisms of conversion of xanthine dehydrogenase to xanthine oxidase in ischemic rat liver and kidney. *Am J Physiol* 254: G753-760, 1988.

84. **McNally JS, Davis ME, Giddens DP, Saha A, Hwang J, Dikalov S, Jo H, and Harrison DG.** Role of xanthine oxidoreductase and NAD(P)H oxidase in endothelial superoxide production in response to oscillatory shear stress. *Am J Physiol Heart Circ Physiol* 285: H2290-2297, 2003.

85. **McNally JS, Saxena A, Cai H, Dikalov S, and Harrison DG.** Regulation of xanthine oxidoreductase protein expression by hydrogen peroxide and calcium. *Arterioscler Thromb Vasc Biol* 25: 1623-1628, 2005.

86. **Metzger JM, Scheidt KB, and Fitts RH.** Histochemical and physiological characteristics of the rat diaphragm. *J Appl Physiol* 58: 1085-1091, 1985.

87. **Mizuno M.** Human respiratory muscles: fibre morphology and capillary supply. *Eur Respir J* 4: 587-601, 1991.

88. **Murrell GA and Rapeport WG.** Clinical pharmacokinetics of allopurinol. *Clin Pharmacokinet* 11: 343-353, 1986.

89. **Nader GA, Hornberger TA, and Esser KA.** Translational control: implications for skeletal muscle hypertrophy. *Clin Orthop Relat Res*: S178-187, 2002.

90. **Nader GA, McLoughlin TJ, and Esser KA.** mTOR function in skeletal muscle hypertrophy: increased ribosomal RNA via cell cycle regulators. *Am J Physiol Cell Physiol* 289: C1457-1465, 2005.

91. **Nishino T.** The conversion of xanthine dehydrogenase to xanthine oxidase and the role of the enzyme in reperfusion injury. *J Biochem* 116: 1-6, 1994.

92. **Nishino T, Okamoto K, Kawaguchi Y, Hori H, Matsumura T, Eger BT, and Pai EF.** Mechanism of the conversion of xanthine dehydrogenase to xanthine oxidase: identification of the two cysteine disulfide bonds and crystal structure of a non-convertible rat liver xanthine dehydrogenase mutant. *J Biol Chem* 280: 24888-24894, 2005.

93. **Pavlovic D and Wendt M.** Diaphragm pacing during prolonged mechanical ventilation of the lungs could prevent from respiratory muscle fatigue. *Med Hypotheses* 60: 398-403, 2003.

94. **Poole DC, Sexton WL, Farkas GA, Powers SK, and Reid MB.** Diaphragm structure and function in health and disease. *Med Sci Sports Exerc* 29: 738-754, 1997.

95. **Powers SK, Demirel HA, Coombes JS, Fletcher L, Calliaud C, Vrabas I, and Prezant D.** Myosin phenotype and bioenergetic characteristics of rat respiratory muscles. *Med Sci Sports Exerc* 29: 1573-1579, 1997.

96. **Powers SK, Kavazis AN, and DeRuisseau KC.** Mechanisms of disuse muscle atrophy: role of oxidative stress. *Am J Physiol Regul Integr Comp Physiol* 288: R337-344, 2005.

97. **Powers SK, Kavazis AN, and McClung JM.** Oxidative stress and disuse muscle atrophy. *J Appl Physiol* 102: 2389-2397, 2007.

98. **Powers SK, Shanely RA, Coombes JS, Koesterer TJ, McKenzie M, Van Gammeren D, Cicale M, and Dodd SL.** Mechanical ventilation results in progressive contractile dysfunction in the diaphragm. *J Appl Physiol* 92: 1851-1858, 2002.

99. **Racz GZ, Gayan-Ramirez G, Testelmans D, Cadot P, De Paepe K, Zador E, Wuytack F, and Decramer M.** Early changes in rat diaphragm biology with mechanical ventilation. *Am J Respir Crit Care Med* 168: 297-304, 2003.

100. **Radell PJ, Remahl S, Nichols DG, and Eriksson LI.** Effects of prolonged mechanical ventilation and inactivity on piglet diaphragm function. *Intensive Care Med* 28: 358-364, 2002.

101. **Rasmussen JT, Rasmussen MS, and Petersen TE.** Cysteines involved in the interconversion between dehydrogenase and oxidase forms of bovine xanthine oxidoreductase. *J Dairy Sci* 83: 499-506, 2000.

102. **Saksela M, Lapatto R, and Raivio KO.** Irreversible conversion of xanthine dehydrogenase into xanthine oxidase by a mitochondrial protease. *FEBS Lett* 443: 117-120, 1999.

103. **Saliaris AP, Amado LC, Minhas KM, Schuleri KH, Lehrke S, St John M, Fitton T, Barreiro C, Berry C, Zheng M, Kozielski K, Eneboe V, Brawn J, and Hare JM.** Chronic allopurinol administration ameliorates maladaptive alterations in Ca2+ cycling proteins and beta-adrenergic hyporesponsiveness in heart failure. *Am J Physiol Heart Circ Physiol* 292: H1328-1335, 2007.

104. **Sassoon CS.** Ventilator-associated diaphragmatic dysfunction. *Am J Respir Crit Care Med* 166: 1017-1018, 2002.

105. **Sassoon CS, Caiozzo VJ, Manka A, and Sieck GC.** Altered diaphragm contractile properties with controlled mechanical ventilation. *J Appl Physiol* 92: 2585-2595, 2002.

106. **Sassoon CS, Zhu E, and Caiozzo VJ.** Assist-control mechanical ventilation attenuates ventilator-induced diaphragmatic dysfunction. *Am J Respir Crit Care Med* 170: 626-632, 2004.

107. **Segal SS, White TP, and Faulkner JA.** Architecture, composition, and contractile properties of rat soleus muscle grafts. *Am J Physiol* 250: C474-479, 1986.

108. **Shanely RA, Coombes JS, Zergeroglu AM, Webb AI, and Powers SK.** Short-duration mechanical ventilation enhances diaphragmatic fatigue resistance but impairs force production. *Chest* 123: 195-201, 2003.

109. **Shanely RA, Van Gammeren D, Deruisseau KC, Zergeroglu AM, McKenzie MJ, Yarasheski KE, and Powers SK.** Mechanical ventilation depresses protein synthesis in the rat diaphragm. *Am J Respir Crit Care Med* 170: 994-999, 2004.

110. **Shanely RA, Zergeroglu MA, Lennon SL, Sugiura T, Yimlamai T, Enns D, Belcastro A, and Powers SK.** Mechanical ventilation-induced diaphragmatic atrophy is associated with oxidative injury and increased proteolytic activity. *Am J Respir Crit Care Med* 166: 1369-1374, 2002.

111. **Sitte N, Dubiel W, and Kloetzel PM.** Evidence for a novel ATP-dependent protease from the rat liver mitochondrial intermembrane space: purification and characterisation. *J Biochem* 123: 408-415, 1998.

112. **Stamler JS and Meissner G.** Physiology of nitric oxide in skeletal muscle. *Physiol Rev* 81: 209-237, 2001.

113. **Stark K, Seubert P, Lynch G, and Baudry M.** Proteolytic conversion of xanthine dehydrogenase to xanthine oxidase: evidence against a role for calcium-activated protease (calpain). *Biochem Biophys Res Commun* 165: 858-864, 1989.

114. **Stirpe F and Della Corte E.** The regulation of rat liver xanthine oxidase. Conversion in vitro of the enzyme activity from dehydrogenase (type D) to oxidase (type O). *J Biol Chem* 244: 3855-3863, 1969.

115. **Stofan DA, Callahan LA, Di MA, Nethery DE, and Supinski GS.** Modulation of release of reactive oxygen species by the contracting diaphragm. *Am J Respir Crit Care Med* 161: 891-898, 2000.

116. **Sultan KR, Henkel B, Terlou M, and Haagsman HP.** Quantification of hormone-induced atrophy of large myotubes from C2C12 and L6 cells: atrophy-inducible and atrophy-resistant C2C12 myotubes. *Am J Physiol Cell Physiol* 290: C650-659, 2006.

117. **Supinski G, Nethery D, Stofan D, Szweda L, and DiMarco A.** Oxypurinol administration fails to prevent free radical-mediated lipid peroxidation during loaded breathing. *J Appl Physiol* 87: 1123-1131, 1999.

118. **Supinski G, Stofan D, Callahan LA, Nethery D, Nosek TM, and DiMarco A.** Peroxynitrite induces contractile dysfunction and lipid peroxidation in the diaphragm. *J Appl Physiol* 87: 783-791, 1999.

119. **Tenhunen R, Marver HS, and Schmid R.** The enzymatic conversion of heme to bilirubin by microsomal heme oxygenase. *Proc Natl Acad Sci U S A* 61: 748-755, 1968.

120. **Thomason DB, Biggs RB, and Booth FW.** Protein metabolism and beta-myosin heavy-chain mRNA in unweighted soleus muscle. *Am J Physiol* 257: R300-305, 1989.

121. **Tobin MJ.** Mechanical ventilation. *N Engl J Med* 330: 1056-1061, 1994.

122. **Van Gammeren D, Falk DJ, Deering MA, Deruisseau KC, and Powers SK.** Diaphragmatic nitric oxide synthase is not induced during mechanical ventilation. *J Appl Physiol* 102: 157-162, 2007.

123. **Van Gammeren D, Falk DJ, DeRuisseau KC, Sellman JE, Decramer M, and Powers SK.** Reloading the diaphragm following mechanical ventilation does not promote injury. *Chest* 127: 2204-2210, 2005.

124. **Vassilakopoulos T.** Ventilator-induced diaphragm dysfunction: the clinical relevance of animal models. *Intensive Care Med* 34: 7-16, 2008.

125. **Vassilakopoulos T and Petrof BJ.** Ventilator-induced diaphragmatic dysfunction. *Am J Respir Crit Care Med* 169: 336-341, 2004.

126. **Vassilakopoulos T, Zakynthinos S, and Roussos C.** Respiratory muscles and ventilatory failure. *Monaldi Arch Chest Dis* 51: 489-498, 1996.

127. **Ventadour S and Attaix D.** Mechanisms of skeletal muscle atrophy. *Curr Opin Rheumatol* 18: 631-635, 2006.

128. **Vina J, Gimeno A, Sastre J, Desco C, Asensi M, Pallardo FV, Cuesta A, Ferrero JA, Terada LS, and Repine JE.** Mechanism of free radical production in exhaustive exercise in humans and rats; role of xanthine oxidase and protection by allopurinol. *IUBMB Life* 49: 539-544, 2000.

129. **Watson AC, Hughes PD, Louise Harris M, Hart N, Ware RJ, Wendon J, Green M, and Moxham J.** Measurement of twitch transdiaphragmatic, esophageal, and endotracheal tube pressure with bilateral anterolateral magnetic phrenic nerve stimulation in patients in the intensive care unit. *Crit Care Med* 29: 1325-1331, 2001.

130. **Waud WR and Rajagopalan KV.** The mechanism of conversion of rat liver xanthine dehydrogenase from an NAD+-dependent form (type D) to an O2-dependent form (type O). *Arch Biochem Biophys* 172: 365-379, 1976.

131. **Yang L, Luo J, Bourdon J, Lin MC, Gottfried SB, and Petrof BJ.** Controlled mechanical ventilation leads to remodeling of the rat diaphragm. *Am J Respir Crit Care Med* 166: 1135-1140, 2002.

132. **Zergeroglu MA, McKenzie MJ, Shanely RA, Van Gammeren D, DeRuisseau KC, and Powers SK.** Mechanical ventilation-induced oxidative stress in the diaphragm. *J Appl Physiol* 95: 1116-1124, 2003.

133. **Zhu E, Sassoon CS, Nelson R, Pham HT, Zhu L, Baker MJ, and Caiozzo VJ.** Early effects of mechanical ventilation on isotonic contractile properties and MAF-box gene expression in the diaphragm. *J Appl Physiol* 99: 747-756, 2005.

134. **Zimmerman BJ, Parks DA, Grisham MB, and Granger DN.** Allopurinol does not enhance antioxidant properties of extracellular fluid. *Am J Physiol* 255: H202-206, 1988.

BIOGRAPHICAL SKETCH

Melissa A. (Deering) Whidden was born in Cortland, New York. She earned a Bachelor of Science degree in exercise science from the University at Buffalo, The State University of New York. Following graduation, she pursued a master's degree in applied physiology and graduated from the University at Buffalo, The State University of New York in 2003. Deciding to focus her career in basic science, Melissa began her doctoral work at the University of Florida in 2003 under the direction of Scott K. Powers. Melissa focused her studies on oxidative stress and proteolysis of the diaphragm muscle during prolonged mechanical ventilation. She received her PhD in 2008.